6th Institute of Space Sciences Summer School: Life Cycle of Dust

3-13 July 2023
Institute of Space Sciences

dust in the early Universe & in extreme environments

Raffaella Schneider
Sapienza Università di Roma

raffaella.schneider@uniroma1.it

Outline of lectures

Lecture 1

- core-collapse SN dust formation and survival
- AGB dust formation
- Type Ia SN
- Smoking quasars: dust formation in super-extreme environments

Lecture 2

- SN vs AGB stars as cosmic dust polluters
- Life after formation: dust reprocessing in the ISM
- modeling dust in galaxy evolution

physical conditions for dust formation

two-steps process:

1. nucleation seed clusters from molecular precursors
2. growth of seed clusters to form grains

the gas must be metal-rich with physical conditions allowing condensation

$T < T_{cond} = 1000 – 2000$ K

$n > 10^9$ cm^{-3}

winds of Asymptotic Giant Branch stars

supernova ejecta

the family of supernovae

core-collapse supernovae

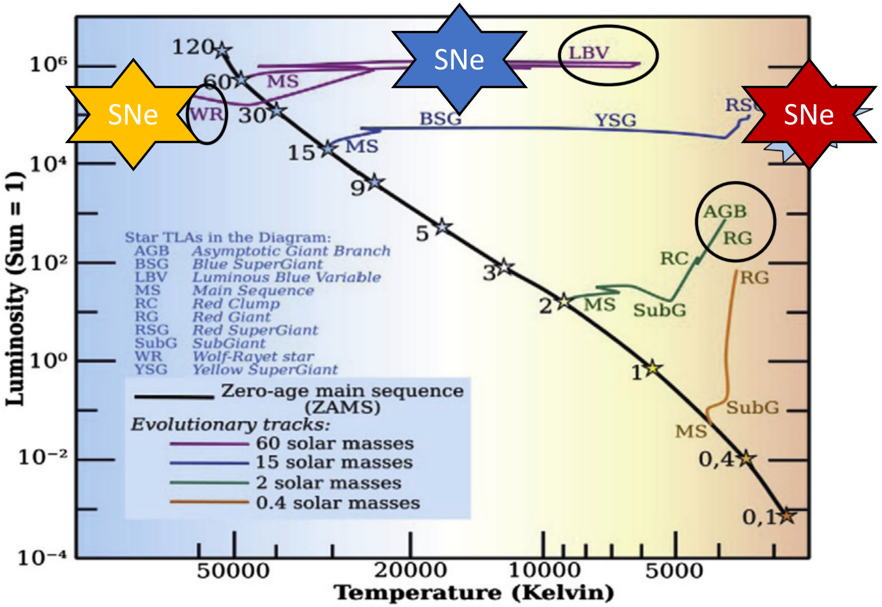

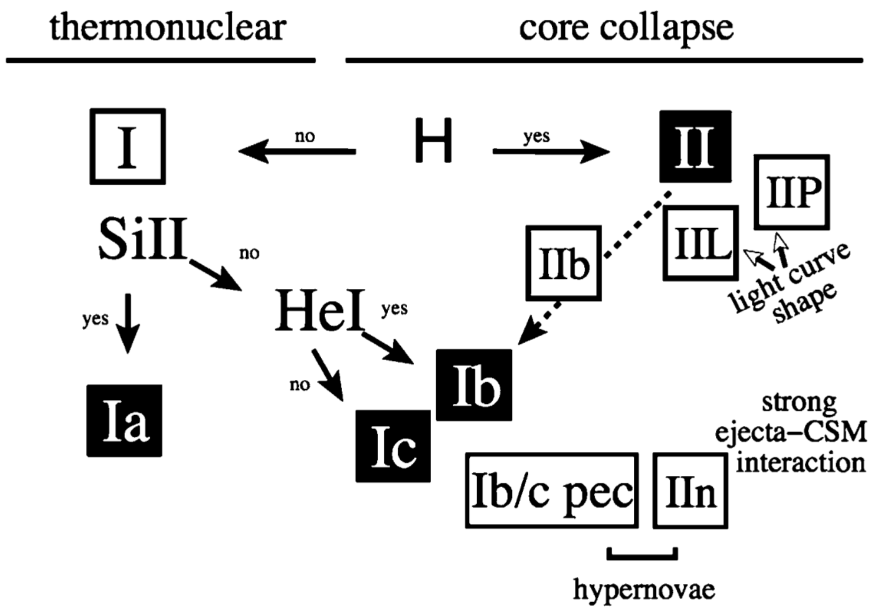

dust formation in supernovae

dust has been observed to form in the ejecta of SN1987A since 450 days after the explosion

(Wooden et al. 1993, Bouchet et al. 2006, Matsuura et al. 2011, Indebetouw et al. 2014)

FIR emission: dust condensed
in the ejecta
M_{dust} = [0.4 - 0.7] M_{sun}
$T_{dust} \approx 20$ K

Matsuura et al. 2011

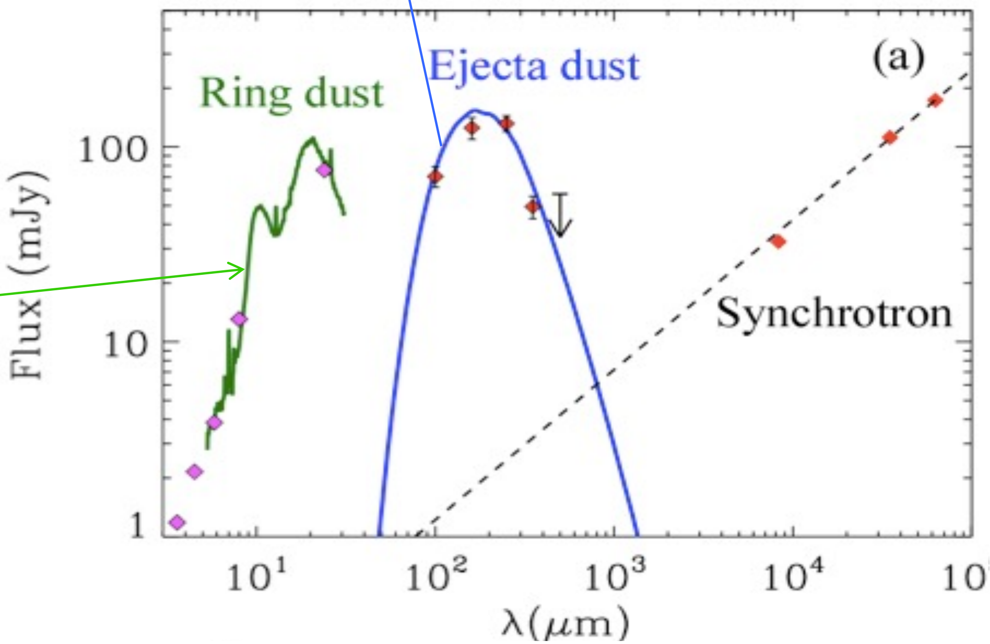

Bouchet et al. 2006

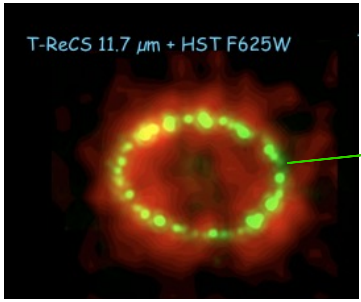

MIR emission: dust in the ring
ejected by the progenitor
$M_{dust} \approx 10^{-6}$ M_{sun}
$T_{dust} \approx 160$ K

models for dust formation in SNe

Kozasa & Hasegawa 1987; Todini & Ferrara 2001; Nozawa et al 2003; Schneider, Ferrara & Salvaterra 2004; Bianchi & Schneider 2007; Chercheneff & Dwek 2010; Fallest et al. 2011; Sarangi & Cherchneff 2013; Marassi+2014, 2015, 2016

1. model for the evolution of the progenitor star (mass, metallicity, rotation)
2. model for the explosion (explosion energy, mass cut/fallback, mixing of the ejecta)
3. grain nucleation

sequence of events in a supernova explosion

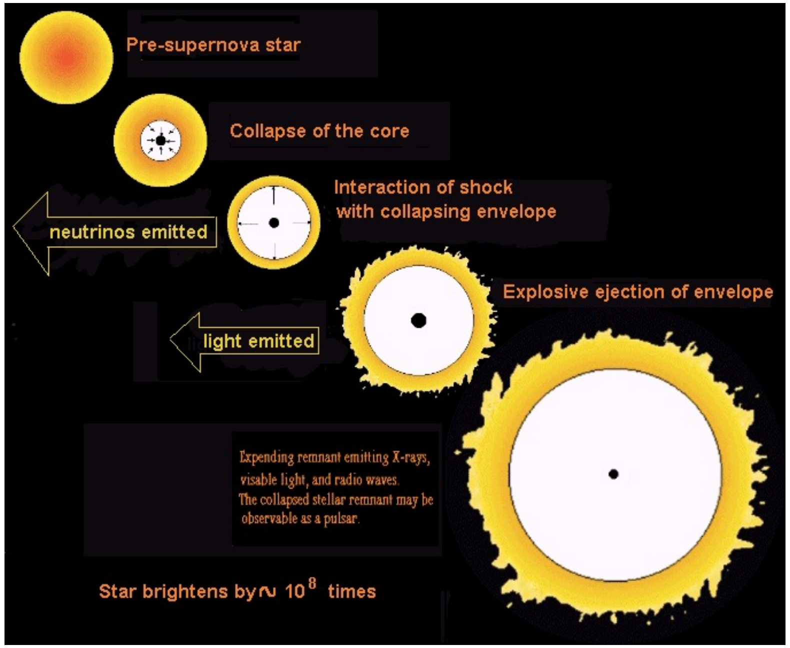

Models use "artifical explosions": energy, mass-cut, M_{Ni56}

- **Explosions @ fixed energy**
- **Calibrated models**

models for dust formation in SNe

Kozasa & Hasegawa 1987; Todini & Ferrara 2001; Nozawa et al 2003; Schneider, Ferrara & Salvaterra 2004;
Bianchi & Schneider 2007; Chercheneff & Dwek 2010; Fallest et al. 2011; Sarangi & Cherchneff 2013; Marassi+2014, 2015, 2016;

1. model for the evolution of the progenitor star (mass, metallicity, rotation)
2. model for the explosion (explosion energy, mass cut/fallback, mixing of the ejecta)
3. grain nucleation

pre-supernova structure

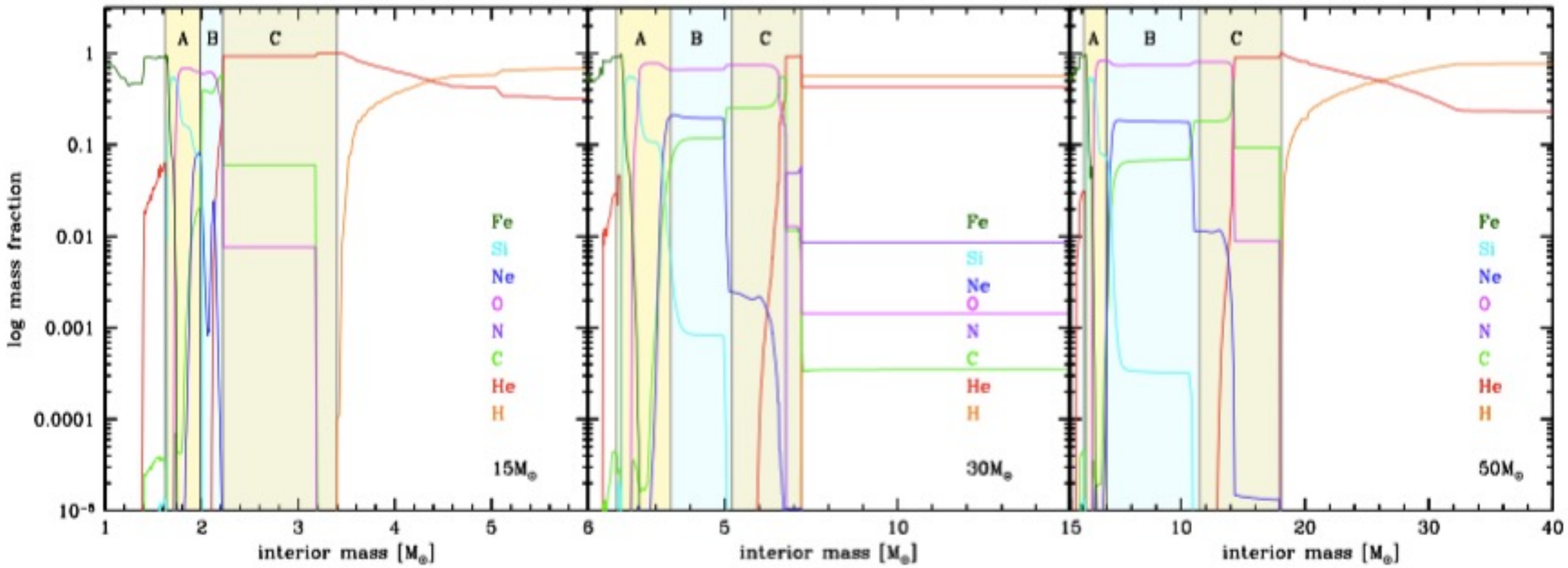

models for dust formation in SNe

Kozasa & Hasegawa 1987; Todini & Ferrara 2001; Nozawa et al 2003; Schneider, Ferrara & Salvaterra 2004;
Bianchi & Schneider 2007; Cherchneff & Dwek 2010; Fallest et al. 2011; Sarangi & Cherchneff 2013; Marassi+2014, 2015, 2016;

1. model for the evolution of the progenitor star (mass, metallicity, rotation)
2. model for the explosion (explosion energy, mass cut/fallback, mixing of the ejecta)
3. grain nucleation

turbulence mixing during ejecta expansion

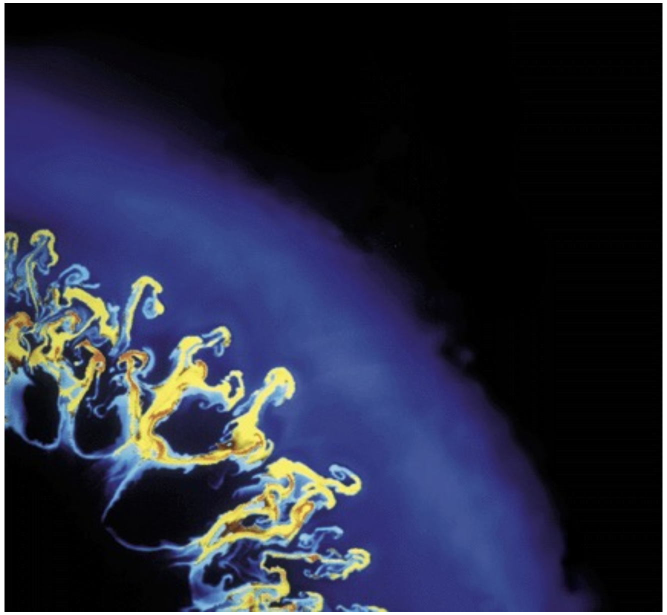

SN1987a: observations of γ-rays from Co^{56} decay 6 months before expected ←→ mixing of heavy elements from innermost to the outer layers

- **fully mixed models**
- **unmixed/stratified models**

modeling supernova dust formation

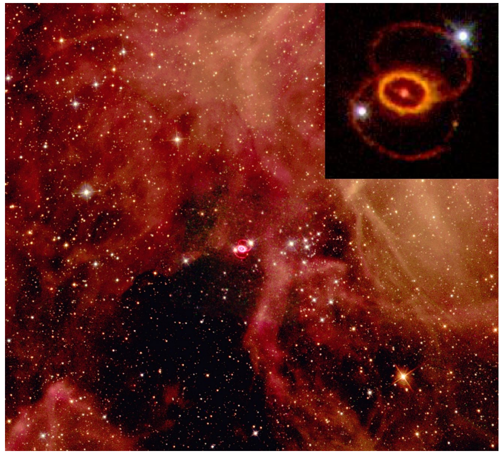

models have followed 3 main approaches:

- Classical Nucleation Theory (CNT) Kozasa et al. (1989, 1991)

Steady state nucleation rate (condensation=evaporation)
Grain growth by accretion of other monomers

do not consider the chemical pathway leading to molecular precursors and seed nuclei

- Kinetic Nucleation Theory (KNT) Nozawa et al. (2003)

Non steady state nucleation rate
Grain growth by accretion of other monomers

- Molecular Nucleation Theory (MNT) or chemical kinetic approach Cherchneff & Lilly (2008), Sarangi & Cherchneff (2012)

chemical pathway proceeds through simultaneous phases of nucleation and condensation
nucleation phase: the formation of molecular and cluster precursors is described by an extended non equilibrium chemical network
condensation phase: small clusters formed in the gas phase condense through coagulation and coalescence to form large grains

SN dust formation – classical nucleation theory

1. gas becomes super-saturated
2. monomers aggregate into seed clusters
3. clusters growth by accretion of other monomers

Steady-state nucleation rate (number of seed clusters formed per unit time and volume):

$$J = \alpha \Omega \left(\frac{2\sigma}{\pi m_k} \right)^{1/2} c_k^2 \exp\left[-\frac{4\mu^3}{27(\ln S)^2} \right],$$

Grain growth rate:

$$\frac{dr}{dt} = \alpha \Omega v_k c_k.$$

sticking coefficent (α)

$\Omega = 4/3\pi a_0^3$ volume of monomer in the condensed phase

σ surface tension of the condensed material

m_k, c_k, v_k mass, concentration and velocity of the monomer

$\mu = 4\pi a_0^2 \sigma/(k_B T)$ parameter, T gas temperature

$\ln S = -\frac{\Delta G_r}{K_B T} + \Sigma_i \nu_i P_i,$ super-saturation ratio

ΔG_r Gibbs free energy of the reaction $\Sigma_i \nu_i A_i = \mathrm{solid}$

A_i = chemical species, ν_i = stoichiometric coefficients, P_i = partial pressures

SN dust formation – classical nucleation theory

Grain properties that are generally included in SN dust formation models
(adapted from Table 8 in Sluder et al. 2016)

Species	Formula	A (10^4 K) [a]	B [a]	σ_{ST} (erg cm^{-2})[a]	r_1 (Å)[a]	ϱ (g cm^{-3})[b]	Condensation nucleus
Iron	Fe	4.8418	16.5566	1800	1.411	7.88069	Fe_4
Silicon	Si	5.36975	17.4349	800	1.684	2.3314	Si_4
Carbon	C	8.64726	19.0422	1400	1.281	2.26507	C_4
Magnesium [c]	Mg	7.0085	18.2386	1100	1.76917	1.74	Mg_4
Forsterite	Mg_2SiO_4	37.24	104.872	436	2.589	3.21394	$Mg_4Si_2O_8$
Iron sulfide	FeS	9.31326	30.7771	380	1.932	4.83256	Fe_4S_4
Silicon carbide	SiC	14.8934	37.3825	1800	1.702	3.22393	Si_2C_2
Alumina	Al_2O_3	18.4788	45.3543	690	1.718	7.97125	Al_4O_6
Enstatite	$MgSiO_3$	25.0129	72.0015	400	2.319	7.97125	$Mg_2Si_2O_6$
Silicon dioxide	SiO_2	12.6028	38.1507	605	2.08	2.64686	Si_2O_4
Magnesia	MgO	11.9237	33.1593	1100	1.646	3.58281	Mg_4O_4
Magnetite	Fe_3O_4	13.2889	39.1687	400	1.805	15.6078	Fe_6O_8
Iron oxide	FeO	11.129	31.985	580	1.682	5.98516	Fe_4O_4
Magnesium sulfide[d]	MgS	9.9783	31.9071	720.69	1.89065	3.30655	Mg_4S_4

[a] The parameters A, B, r_1, and σ are from Nozawa et al. (2003) for all grain species except Mg and MgS.
[b] The mass density was taken to be the mass of a monomer divided by $4\pi a_1^3/3$.
[c] For Mg we simply averaged the parameters for C and Si.
[d] The parameters for MgS were scaled from those for MgO using the FeS to FeO parameter ratios.

SN dust formation – classical nucleation theory

thanks to its simplicity, CNT has been applied to perform systematic explorations of dust condensation in 1D spherically symmetric SN explosion models with varying progenitornmass, metallicity, rotation rate, explosion energy, and supernova type

- core collapse supernova grid by Woosley & Weaver (1995), progenitors masses [12 - 40] M_{sun} and metallicities Z = 0, 10^{-4} Z_{sun}, 10^{-2} Z_{sun}, 1 Z_{sun}
(Todini & Ferrara 2001; Bianchi & Schneider 2007, including the reverse shock)

- pair-instability supernova grid by Heger & Woosley (2002)), progenitors masses [140 - 260] M_{sun} and metallicity Z = 0
(Schneider et al., 2004)

- faint SN explosions grid built from Limongi & Chieffi (2012) tailored to reproduce surface elemental abundances of iron-poor C-enhanced milky way halo stars, progenitor masses [13 – 80] M_{sun}, initial metallicity Z = 0
(Marassi et al., 2014)

- core-collapse supernova grid by Limongi & Chieffi (2018), progenitors mass [13 - 120] M_{sun} with initial equatorial rotational velocities of v = 0 and v = 300 km/s and metallicities, Z = 10^{-3} Z_{sun}; 10^{-2} Z_{sun}; 10^{-1} Z_{sun}; 1 Z_{sun}
(Marassi et al. 2019)

SN dust formation – kinetic nucleation theory

Non steady – state nucleation rate
condensation rate of seed clusters of n > 2 atoms is computed from kinetic theory
Nozawa et al. (2003)

- SNIIp with progenitor masses [13 – 20] M_{sun}, metallicity Z = 0

- pair instability SN explosions with progenitor masses of 170 M_{sun} and 200 M_{sun}, metallicity Z = 0
(Nozawa et al. 2003)

- SNIb (similar to SN2006jc), SNIIb (similar to Cas A)
(Nozawa et al. 2008)

- core collapse supernovae grid from Fryer et al. (2008) with progenitor masses 15, 20, and 25 M_{sun} and wide range of explosion energies
(Brook et al. 2022)

SN dust formation – common findings of CNT/KNT

strong dependence on explosion energy and mass of the outer H-rich envelope:

- less massive outer envelope → larger expansion velocities of the He-core → rapid decrease in ejecta T, n → dust formation occurs earlier, the total dust mass formed is comparable but grain sizes are strongly reduced

- less energetic explosion → slower evolution of the ejecta → delayed dust formation → more massive grains

explosive nucleosynthesis depends on the explosion energy: dust composition is also affected

SN dust formation – molecular nucleation theory

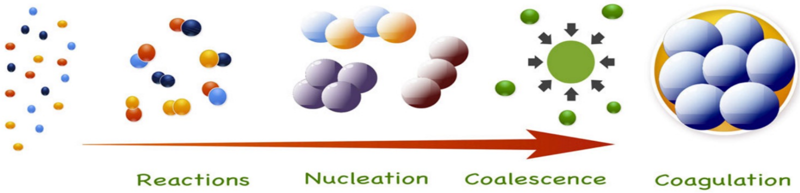

Sarangi+2018

exploration of the nucleation phase (formation of molecules and early dust precursors)

- pair instability SN explosion with progenitor mass of 170 M_{sun} metallicity Z = 0
(Cherchneff & Lilly 2008)

- SNIIp with progenitor mass 20 M_{sun}, metallicity Z = 0
(Cherchneff & Dwek 2009, Cherchneff & Dwek 2010)

- SNIIp with progenitor mass 12, 15, 19, and 25 M_{sun}, metallicity Z = Zsun
(Sarangi & Cherchneff 2013)

inclusion of the condensation phase (coagulation)

- SNIIp with progenitor mass 12, 15, 19, and 25 M_{sun}, metallicity Z = Zsun
(Sarangi & Cherchneff 2015)

SN dust formation: condensation/growth

cluster collisions with monomers are more frequent than cluster collisions with clusters because monomers are lighter and have larger thermal velocities

(Lazzati & Heger 2016)

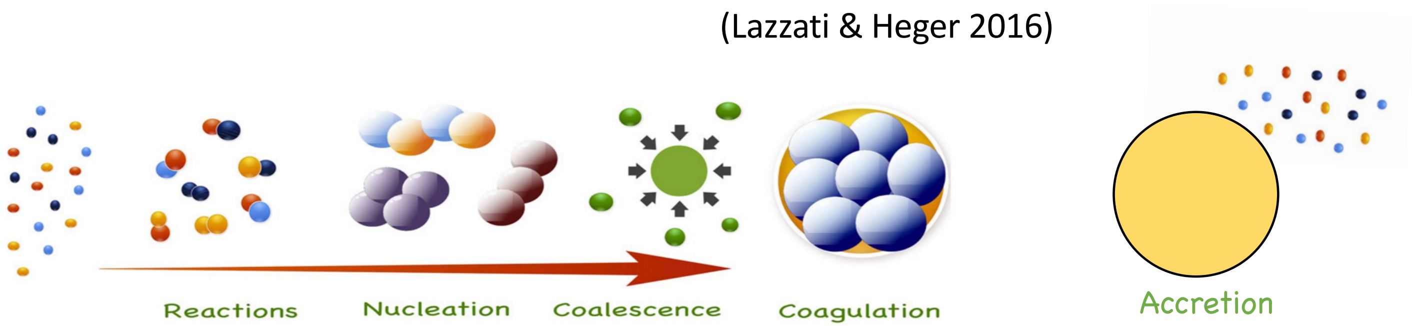

Sarangi+2018

Sluder et al. (2016) apply MNT in a framework where the nucleation phase is joined to the condensation phase through both coagulation and grain growth

they modelled dust formation in SN1987A adopting a 25 M_{sun} core-collapse SN model

SN dust formation: model comparison

total dust mass formed for different SN progenitor masses, $Z = Z_{sun}$ and $E_{expl} = 10^{51}$ erg

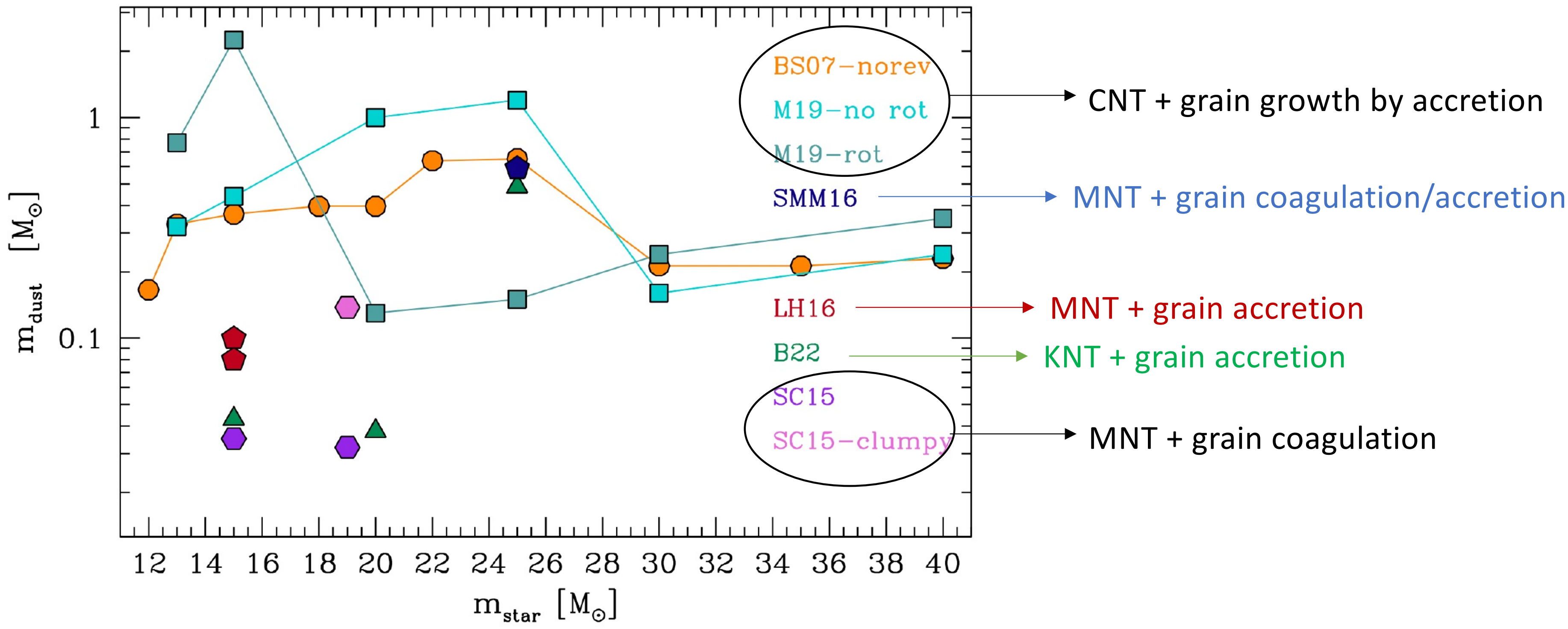

SN dust formation: model comparison

total dust mass formed for different SN progenitor masses, $Z = Z_{sun}$ and $E_{expl} = 10^{51}$ erg

most efficient dust producers:
SNe from low-mass rotating progenitors

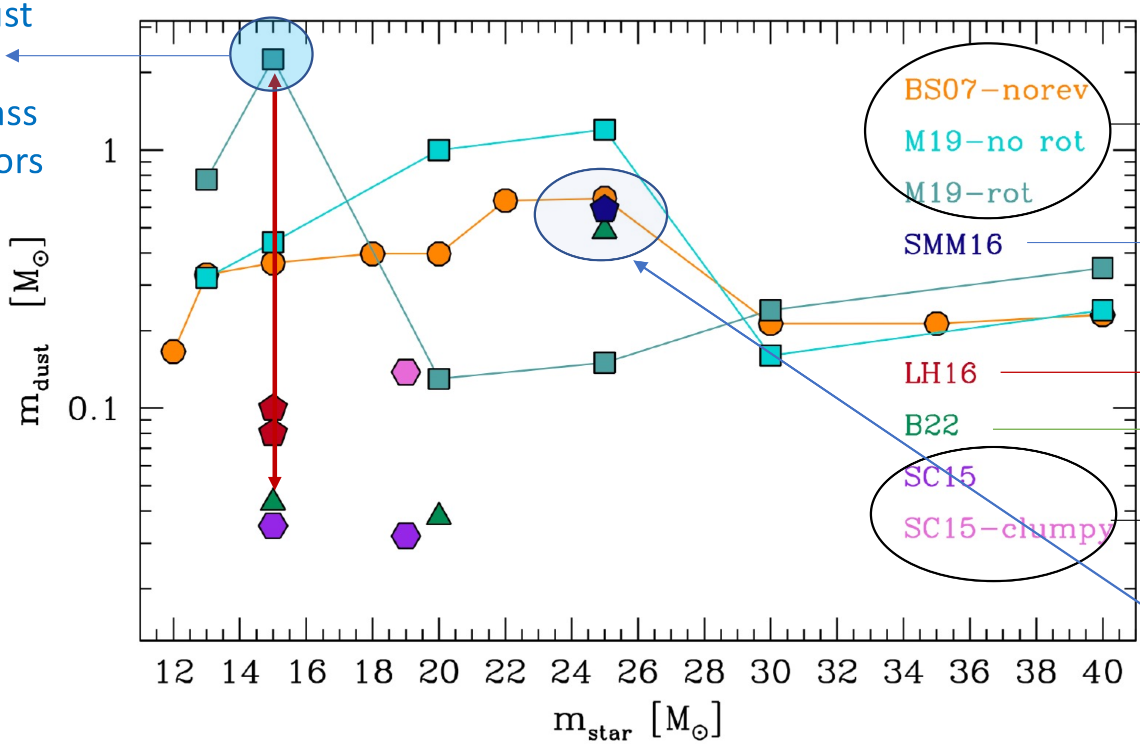

CNT + grain growth by accretion

MNT + grain coagulation/accretion

MNT + grain accretion

KNT + grain accretion

MNT + grain coagulation

- predicted dust masses are scattered between ≈ 0.03 M_{sun} to 1-2 M_{sun}
- models based on CNT tend to predict larger dust masses than models based on KNT/MNT but see Sluder+2016

SN dust formation: model comparison

total dust mass formed for different SN progenitor masses, $Z = Z_{sun}$ and $E_{expl} = 10^{51}$ erg

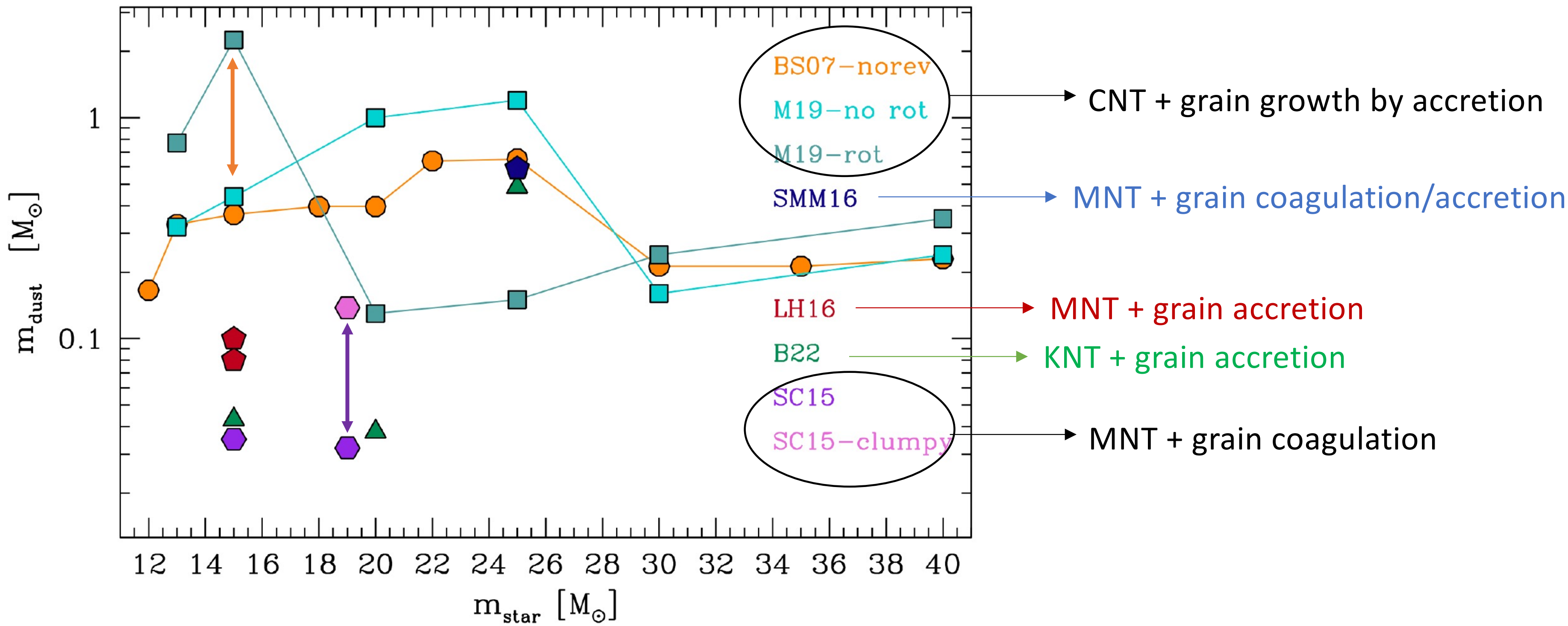

- even adopting the same approach (CNT), m_{dust} depends on SN model and progenitor rotation rate (when $m_{star} < 25\ M_{sun}$)
- clumpy vs homogeneous ejecta leads to an increase by ≈ 0.5 dex in m_{dust}

SN dust formation: comparing dust composition

carbon: carbon grains

silicates:
enstatite $MgSiO_3$
fosterite Mg_2SiO_4
silicon carbide SiC
silicon dioxyde SiO_2
pure silicon Si

other:
Alumina Al_2O_3
magnetite Fe_3O_4
solid iron Fe
iron sulfide FeS,
iron oxyde FeO

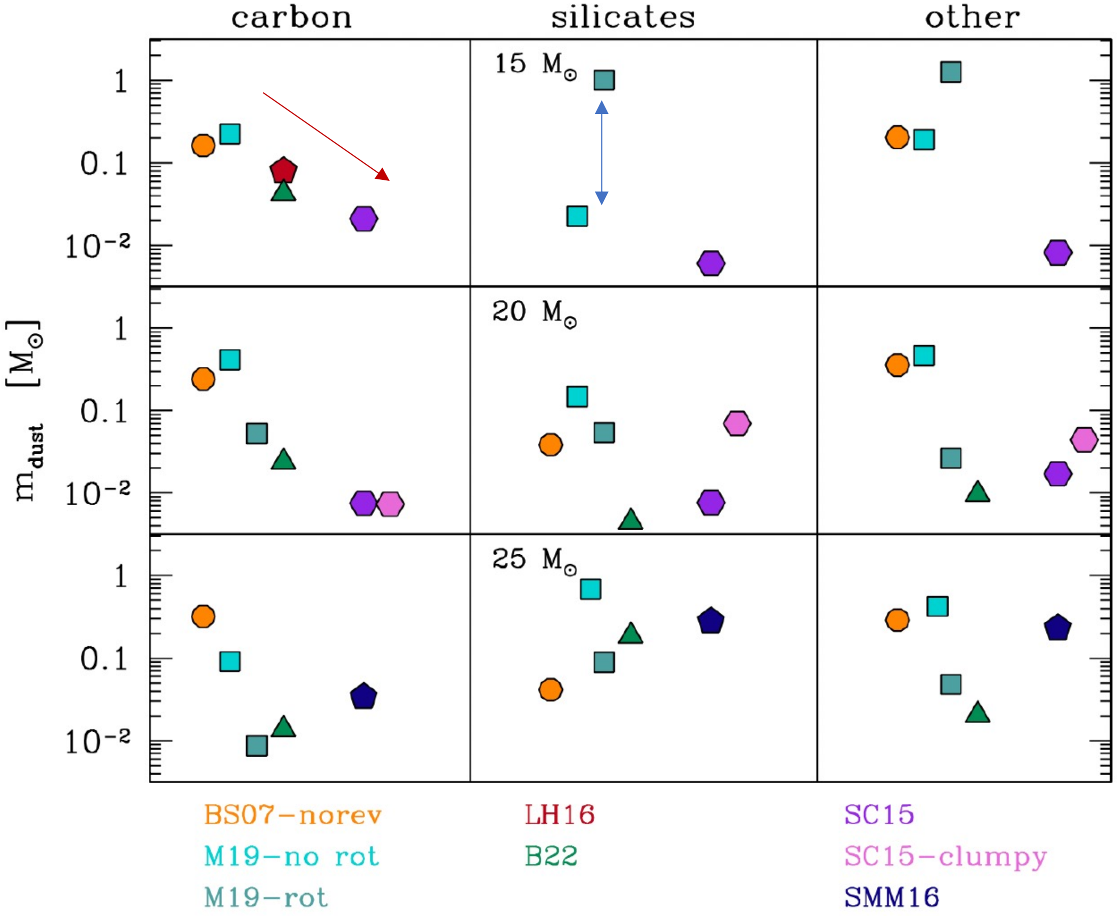

- a large variety of species form in all the models
- compositon depends on the nucleation model
- for low mass progenitors silicates and othe dust species depends on rotation

comparing grain sizes: the case of SN1987A

19 M_{sun} clumpy SN model Sarangi & Cherchneff(2015)

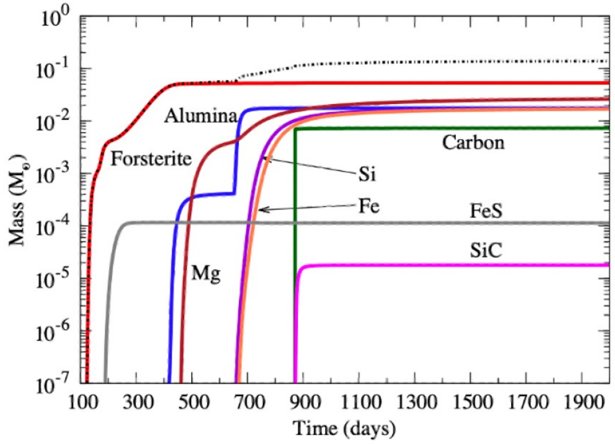

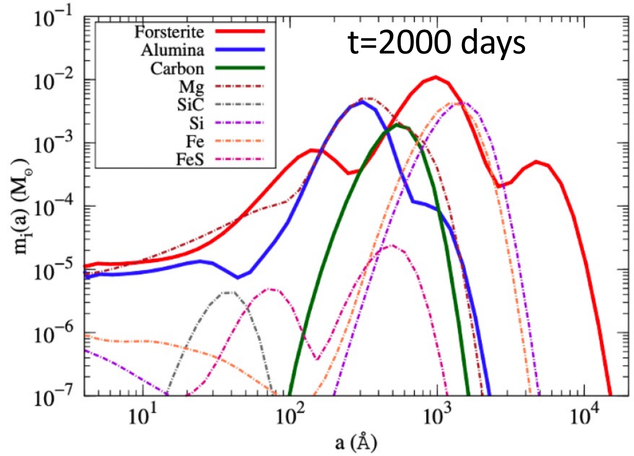

m_{dust} = 0.14 $M_{sun.}$ a ≈ 200 A – 5 10^3 A

dust formation starts 100 -200 days after the explosion

similar time dependence BUT larger dust masses and radii in Sluder+2016

? effect of accretion ?
? different SN ejecta model ?

20 M_{sun} SN model Sluder et al (2016)

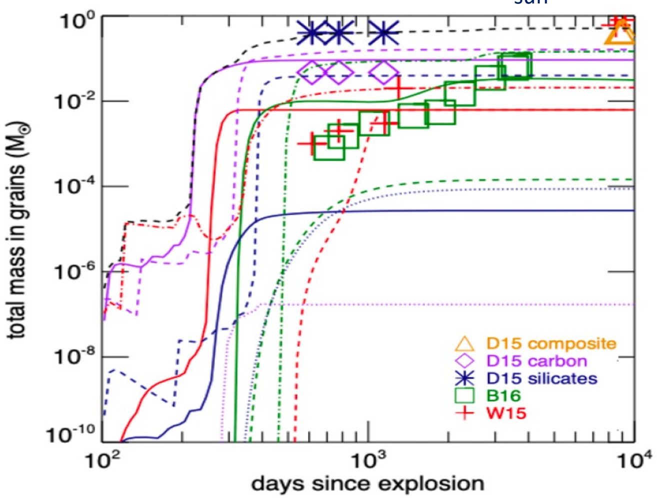

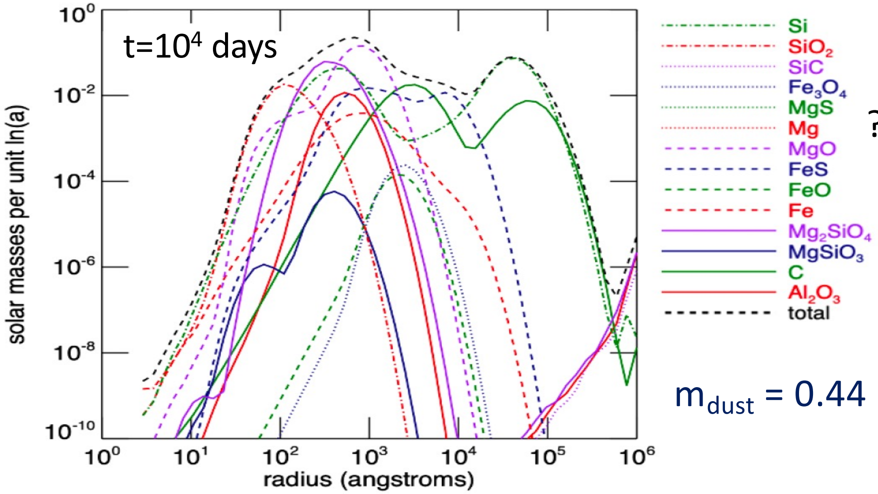

m_{dust} = 0.44 $M_{sun.}$ a ≈ 200 A – 5 10^4 A

comparing models and observations: the case of SN 1987A

20 M_{sun} SN model Sluder et al (2016)

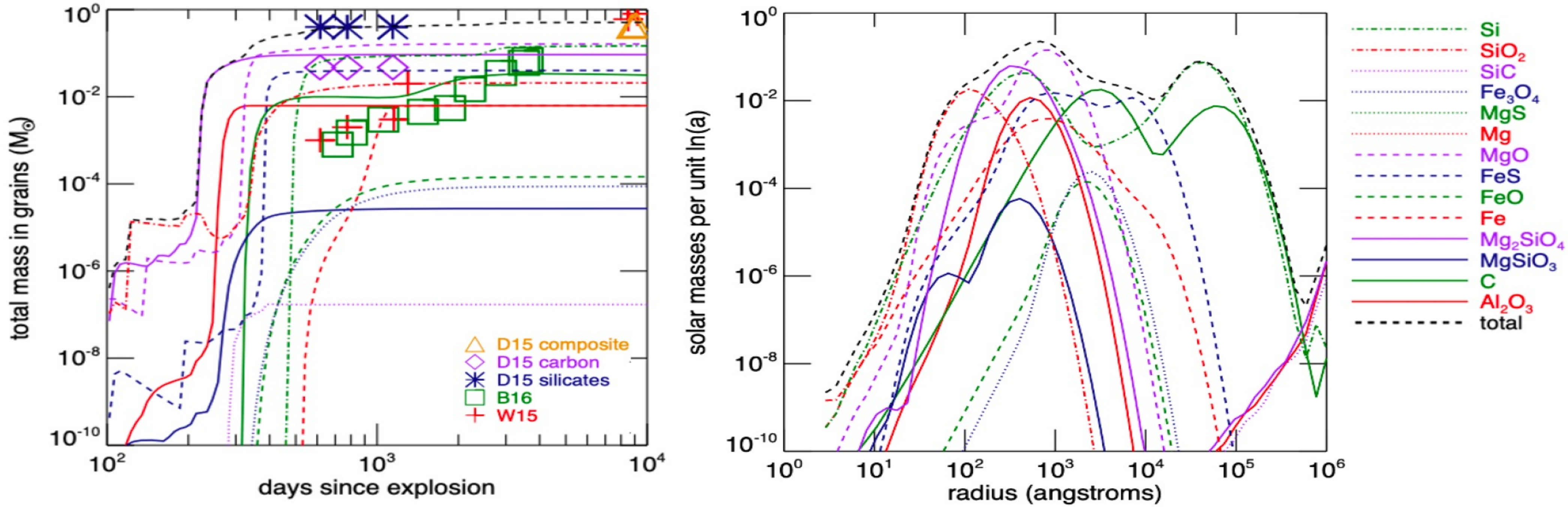

observationally estimated mdust are obtained by fitting the observed Spectral Energy Distribution (SED) at different epochs using 3D RT models (Wesson+2015, W15) and/or blueshifting of the line profiles (Bevan & Barlow 2016, B16), or simpler analytical models (Dwek+2015 D15)

more gradual increase in observed dust mass than predicted by models (W15, B16) or prompt formation but large fraction of dust hidden In optically thick clouds (D15)?

dust processing and survival in SN remnants

not all the dust newly formed in SN ejecta reaches the interstellar medium (ISM) due to processing by the reverse shock (RS)

2D simulations of clumpy ejecta (density contrast 100)

lognormal size distribution with peak 3000 A

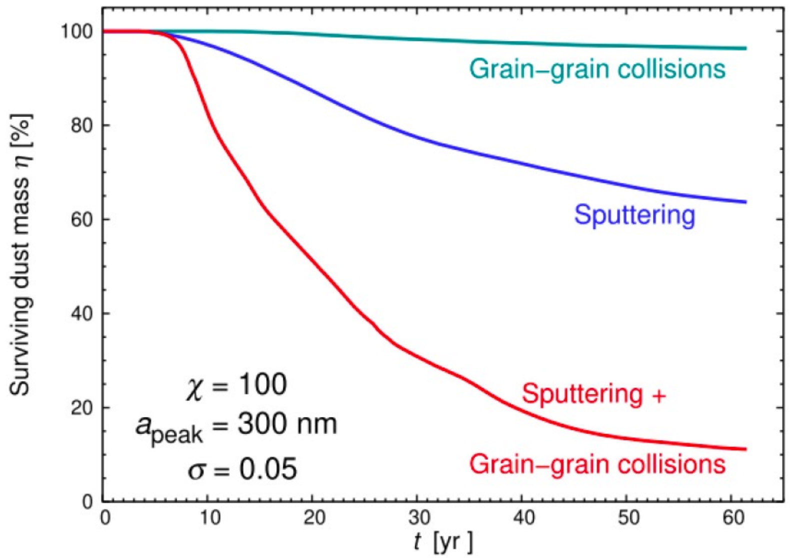

Kirchschlager et al. (2019)

a grain can undergo different destructive processes:

sputtering and grain-grain collisions can be synergistic processes as grain fragments resulting from collisions can be eroded in a more efficient way

Bocchio+2016

dust processing and survival in SN remnants

effective dust yield is the dust mass that survives the RS depends on the initial position and size of the grains

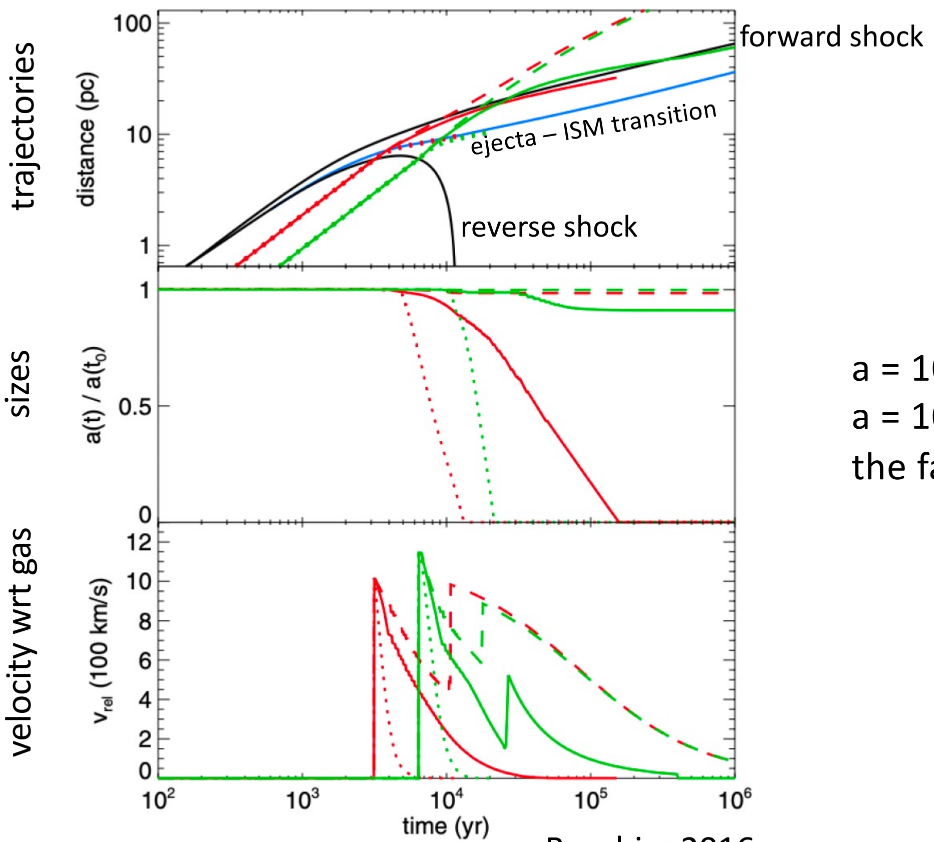

Bocchio+2016

Green: grains with initial position = 0.25 radius of the ejecta
Red: grains with initial position = 0.5 radius of the ejecta

.... a = 10^2 A
___ a = 10^3 A
----- a = 10^4 A

a = 10^4 A grains cross the forward shock unaffected
a = 10^2 A grains are stopped and destroyed
the fate of a = 10^3 A grains depends on their initial position

dust processing in SN remnants: late time evolution

2D simulation of a clumpy (x100) SN ejecta (Slavin et al. 2020)

density distribution and grain position

fractional mass reduction in the ISM

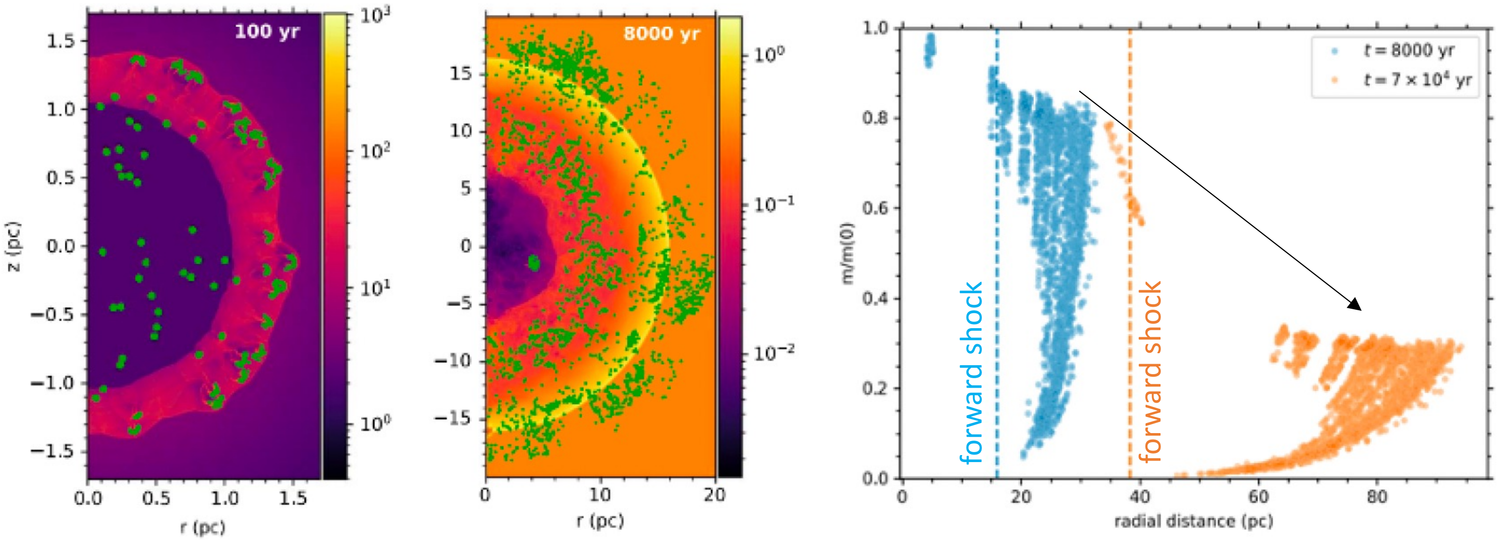

a = 10^4 A grains

substantial mass loss continues to occur at later times, as the grains are slowed in the ISM

surviving mass fraction

paper	η [%]	t [10^3 yr]	χ	processes	a_{grain} [nm]	SN type	n_{ISM} [cm^{-3}]
Bianchi & Schneider (2007)	2 – 20	[40 – 80]	1	sp, sub	[2 - 60]	cc SNe[a]	0.06, 0.6, 6
Nozawa et al. (2007)	0 – 0.4	[300 – 2000]	1	sp, sub	[0.2 - 100]	Pop III cc SNe[b]	0.1, 1, 10
	0.004 – 0.8	[300 – 2000]	1	sp, sub	[0.2 - 500]	Pop III cc SNe[c]	0.1, 1, 10
	0 – 0.45	[700 – 5000]	1	sp, sub	[0.2 - 300]	Pop III PISN[d]	0.1, 1, 10
Nath et al. (2008)	< 0.8 – 1	[1 – 4]	1	sp	[0.1 - 300]	cc SN[e]	0.6
Silvia et al. (2010)	0.05 – 0.89	$\gtrsim 1$	100, 1000	th sp	[0.2 - 500]	cloud-crush[f]	-
Silvia et al. (2012)	0.02 – 1	$\gtrsim 1$	1000	th sp	[0.2 - 500]	cloud-crush[g]	-
Marassi et al. (2015)	3 – 50	~ 10	1	sp, sub	[1 - 500]	Pop III cc SNe[h]	0.06, 0.6, 6
	13, 28, $\lesssim 1$	~ 0.0615, 0.1, 0.2	100, 300, 1000	sp, sub, gg	1000 [0.02] carb	cloud-crush[q]	1
	6, 15, 37	~ 0.0615, 0.1, 0.2	100, 300, 1000	sp, sub, gg	20 [0.02] sil	cloud-crush[q]	1
	8, 3, 2	~ 0.0615, 0.1, 0.2	100, 300, 1000	sp, sub, gg	100 [0.02] sil	cloud-crush[q]	1
	$\lesssim 1$	~ 0.0615, 0.1, 0.2	100, 300, 1000	sp, sub, gg	1000 [0.02] sil	cloud-crush[q]	1
Slavin et al. (2020)	0.4, 2	70	100	sp	40 sil, carb	SN-IIb[r]	0.3 - 1.5
	3, 35	70	100	sp	100 sil, carb	SN-IIb[r]	0.3 - 1.5
	20, 70	70	100	sp	250 sil, carb	SN-IIb[r]	0.3 - 1.5
	40, 82	70	100	sp	395 sil, carb	SN-IIb[r]	0.3 - 1.5
	60, 90	70	100	sp	625 sil, carb	SN-IIb[r]	0.3 - 1.5
	3, 35	70	100	sp	LN1 sil, carb	SN-IIb[r]	0.3 - 1.5
	4, 32	70	100	sp	PL1 sil, carb	SN-IIb[r]	0.3 - 1.5
Kirchschlager et al. (2022)	0 - 10	0.1	300	sp, gg, B	20 [0.02]	cloud-crush[s]	1
	0 - 10	0.1	300	sp, gg, B	100 [0.02]	cloud-crush[s]	1
	0 - 70	0.1	300	sp, gg, B	1000 [0.02]	cloud-crush[s]	1

there exist physical conditions for which a moderate to large fraction (> 10 - 30 %) of SN dust is able to survive enriching the ISM. These are more easily met when clumpy ejecta, with moderate to high overdensities, produce grains with initial sizes & 100 nm, and/or explode in a very tenuous ambient medium, and when the magnetic field is very low or absent.

Micelotta et al. (2016), Schneider & Maiolino in prep

dust processing in SN remnants: comparison with observations

compilation of dust mass determinations for Cas A and Crab SNR

	Cas A	340 [yr]	
Reference	$M_d [M_\odot]$	T_d[K]	Notes
Barlow et al. (2010)	0.075	35	silicates
Arendt et al. (2014)	$\lesssim 0.1$	cold	undetermined
De Looze et al. (2017)	[0.3 – 0.5]	[30 - 32]	silicates
	[0.4 – 0.6]		50% silicates, 50% carbonaceous grains
Bevan et al. (2017)	1.1		50nm 50% silicates, 50% carbonaceous grains
Niculescu-Duvaz et al. (2021)	0.99 ± 0.1		[50 – 200]nm 50% silicates, 50% carbonaceous grains
	0.99 ± 0.1		[200]nm 75% silicates, 25% carbonaceous grains
Priestley et al. (2022)	[0.6 – 0.8]	cold	100nm silicate grains
	~ 0.13	cold	100nm 50% silicates, 50% carbonaceous grains
	Crab	969 [yr]	
Reference	$M_d [M_\odot]$	T_d [K]	Notes
Gomez et al. (2012)	$0.24^{+0.32}_{-0.08}$	[25 - 34]	silicate grains
	0.11 ± 0.01	[32 - 36]	carbonaceous grains
	[0.14 + 0.08]		silicate + carbonaceous grains
Temim & Dwek (2013)	$0.19^{+0.010}_{-0.003}$	56 ± 2	≤ 100nm carbonaceous grains
	0.13 ± 0.01	[23 - 55]	≤ 5000nm silicate grains
Owen & Barlow (2015)	[0.18 – 0.27]	-	[50-700]nm clumped carbonaceous grains
	[0.98 – 1.10]	-	[10-900]nm clumped silicates
	[0.38 – 0.47] + [0.11 – 0.13]	-	[10-1000]nm silicates + carbonaceous grains
De Looze et al. (2019)	[0.032 – 0.049]	41 ± 3	1000 nm carbonaceous grains
Nehmé et al. (2019)	0.056 ± 0.037	42.06 ± 1.14	
Priestley et al. (2020)	0.026 – 0.039	-	[1-1000]nm carbonaceous grains
	0.076 – 0.218	-	[1-1000]nm silicate grains
Chastenet et al. (2022)	< [0.0002 – 0.0036]	~ [40 – 70]	[100-5000]nm carbonaceous grains
	< [0.026 – 0.059]	~ [30 – 50]	[100-5000]nm silicate grains

dust mass determinations are affected by the adopted dust composition, optical constants, and size distribution

Young Cas A [340 yr]
M_{dust} = [0.3 – 1] M_{sun}

Old Crab [960 yr]
M_{dust} = [0.026 – 0.049] M_{sun}

Niculescu-Duvaz et al. (2022)

dust processing in SN remnants: comparison with observations

time evolution of dust mass in SNR: models vs obs

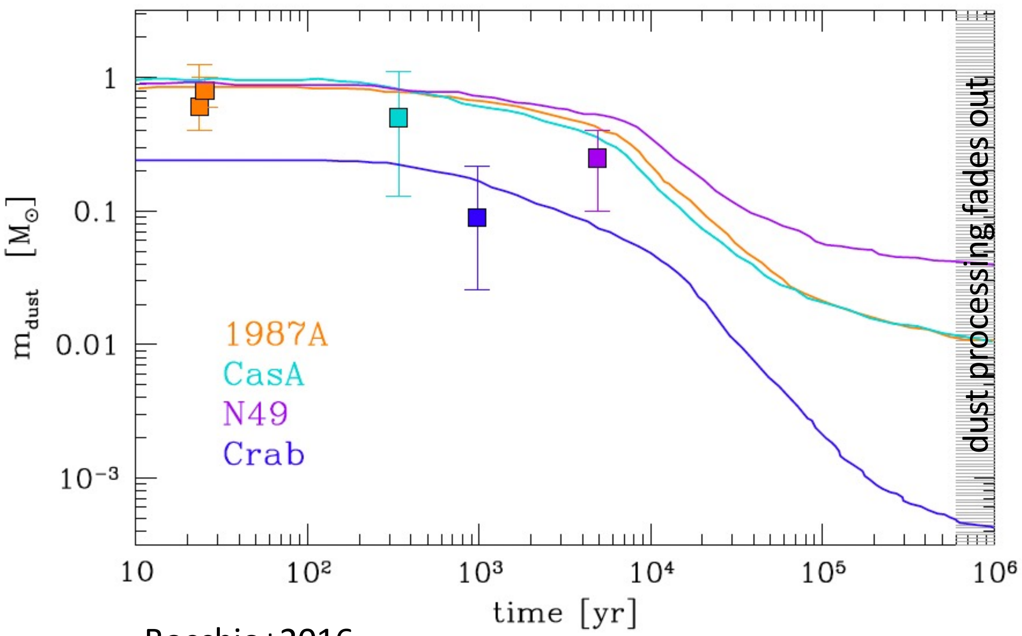

Bocchio+2016

reasonable agreement with observations but extrapolating to t > 10^4 yr leads to very small effective dust yields

see also: Bianchi & Schneider (2007); Nozawa et al. (2010); Biscaro & Cherchneff (2016)

dust formation in AGB stars

see the lecture by
Ciska Kemper on Wednesday July 5

atmospheric levitation by pulsation induced shock waves and radiative acceleration of dust grains which form in the atmosphere

- **full hydrodynamical simulations** with self-consistent dust formation and multi-wavelength radiative transfer (Hofner & Olofsson, 2018)

  extensive grids of C-stars (Mattsson et al., 2010; Eriksson et al., 2014) and M-stars (Bladh et al., 2019) have been computed using the DARWIN code (Hofner et al., 2003, 2016)

- **stationary, spherically symmetric wind** (Ferrarotti & Gail, 2006) with parameters calibrated on observations using:

  synthetic stellar models (simple parametric approximations to describe the changing composition of the atmosphere)
  Ferrarotti & Gail (2006); Zhukovska & Gail (2008); Gail et al. (2009); Zhukovska & Gail (2008); Gail et al. (2009)

  semi-synthetic stellar models (the stellar structure equations are integrated from the atmosphere down to the bottom of the hydrogen-burning shell, using the characteristic quantities at the first thermal pulse obtained from PARSEC stellar models)
  Nanni et al. (2013, 2016, 2018)

  fully numerical stellar models (based on the ATON code, which integrates the evolution of the stars from their pre-main-sequence phase until the almost complete ejection of their external mantle.
  Ventura et al. 2012°, 2012b, 2019; Di Criscienzo et al. 2013 ; Dellì'Agli et al. 2017, 2019)

dust formation in AGB stars

importance of time dependent physical/chemical properties of stellar atmospheres:

Third Dredge Up (TDU)

follows each thermal pulse and that transport the products of the He-burning shell to the stellar surface, transforming the original O-star in a C-star

Hot Bottom Burning (HBB)

proton-capture nucleosynthesis at the base of the outer envelope, that favours the conversion of C to N by the CN-cycle and the reconversion of the C-rich to an O-rich atmosphere

dust formation in AGB stars: model comparison

Zhukovska & Gail (2008)

Nanni et al. (2014, 2015)

Ventura et al. (2012, 2018)

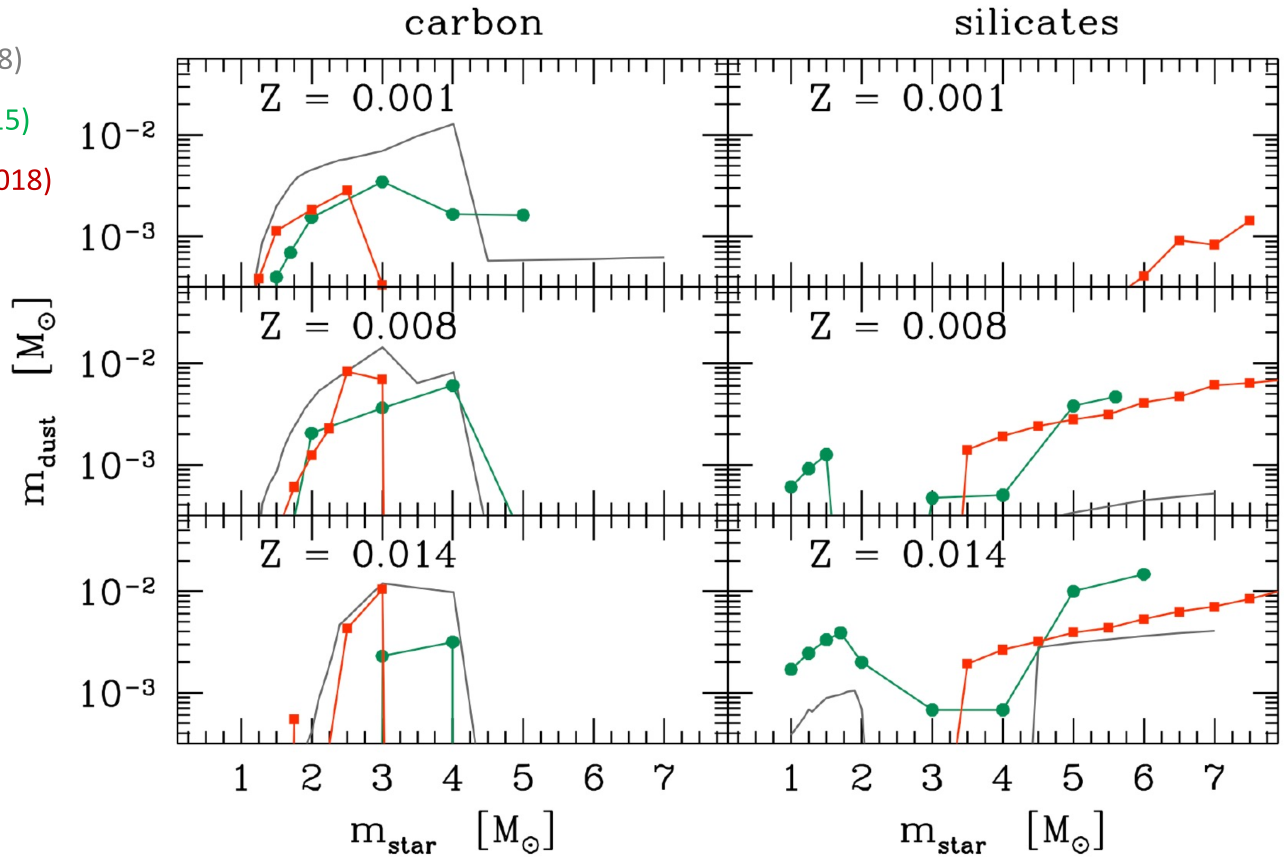

Common trends:

- carbon grains are more efficiently produced by low mass AGB stars;
- silicates are produced in higher mass AGB stars;
- siilicate dust production is very sensitive to metallicity

large variations for individual stars → effects of TDU/HBB

AGB stars: transition from silicate to carbon dust production

ATON dust models Ventura et al. 2012a, 2012b, 2019; Di Criscienzo et al. 2013 ; Dellì'Agli et al. 2017, 2019)

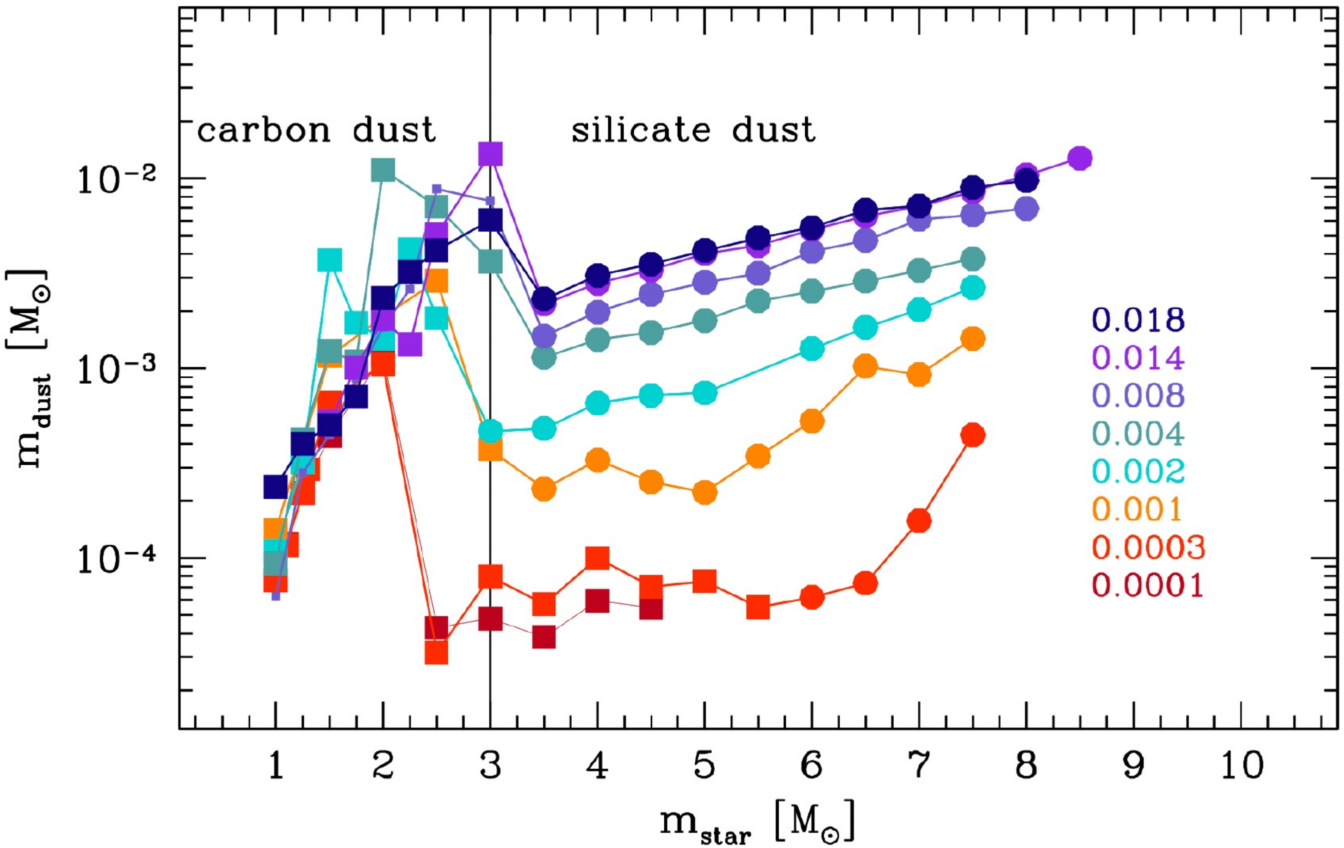

stars with m_{star} < 3-3.5 M_{sun} do not experience HBB (T < 40 MK) and produce carbon dust

carbon dust production from AGB stars requires > 300 Myr from the onset of star formation

at t < 300 Myr AGB with m_{star} > 3-3.5 M_{sun} produce silicate dust, with efficiency that depends on metallicity

AGB dust production: confronting models and observations

global AGB dust production rates (DPR) at the present time for galaxies with different masses and metallicities

Name	Log $M_{star}/M_{\odot}$	$Z/Z_{\odot}$	SFR	DPR	dominant species	relevant data	reference
Sextan A	6.6	0.07	0.006	6×10^{-7}	90% [0.1 – 0.2] μm carbon 10% [0.05 – 0.07] μm silicates	WHIRC/WIYN[c], Spitzer[b]	Dell'Agli et al. (2019b)
IC10	8.5	0.2	0.01	7×10^{-6}	~ 0.15 μm carbon	WFCAM/UKIRT[a], Spitzer[b]	Dell'Agli et al. (2018)
IC1613	6.7	0.05	0.08	5×10^{-5}	80% [0.003 – 0.18] μm carbon 20% [0.001 – 0.08] μm silicates	WFCAM/UKIRT[d], Spitzer[b]	Dell'Agli et al. (2016)
LMC	9.04	0.6	0.39	4.5×10^{-5}	85% [0.05 – 0.2] μm carbon 15% 0.1 μm silicates	Spitzer[e]	Dell'Agli et al. (2015a)
LMC	9.04	0.6	0.39	1.77×10^{-5}	carbon	mixed catalogues[f,g,h]	Nanni et al. (2019)
SMC	8.5	0.2	0.03			Spitzer[i]	Dell'Agli et al. (2015b)
SMC	8.5	0.2	0.03	2.56×10^{-6}	carbon	mixed catalogue[h,l]	Nanni et al. (2019)

time-dependent grids of AGB stars + RT modeling → source-by-source comparison as well as global DPR

- current DPRs depend strongly on galaxy properties and are dominated by carbon grains produced by $m_{star} < 3\ M_{sun}$
- silicate DPRs are likely more common in metal-rich young starburst galaxies, with stellar populations younger than 300 Myr

SNIa do not produce dust

no evidence for dust condensation in type Ia SNe has been found to date
(Blair et al., 2007; Gomez et al., 2012; Williams et al., 2013;…)

Why?

- unfavourable conditions in the ejecta (compared to type Iip SNe): larger expansion velocity (10^4 km/s, 1 dex larger)
→ lower density → less efficient grain condensation and smaller grains ($a < 0.01$ μm)

- larger abundance of ^{56}Ni (0.6 M_{sun}, 1 dex larger) → larger flux of energetic electrons released in the radioactive decay
→ prevent the formation of large molecular precursors

- effects of reverse shock are more destructive due to lack of hydrogen envelope → reverse shock sweep dust forming region at earlier times (< 500 yr) compared to hydrogen-envelope-retaining Sne (> 1000 yr), ejecta density is higher → higher sputtering

between 3 10^{-4} M_{sun} - 0.2 M_{sun} of dust can form in SNIa ejecta BUT < 10^{-5} M_{sun} survive on t > 1 Myr

Nozawa et al. (2011)

interesting implications for the origin of iron grains Dwek (2016)

smoking quasars

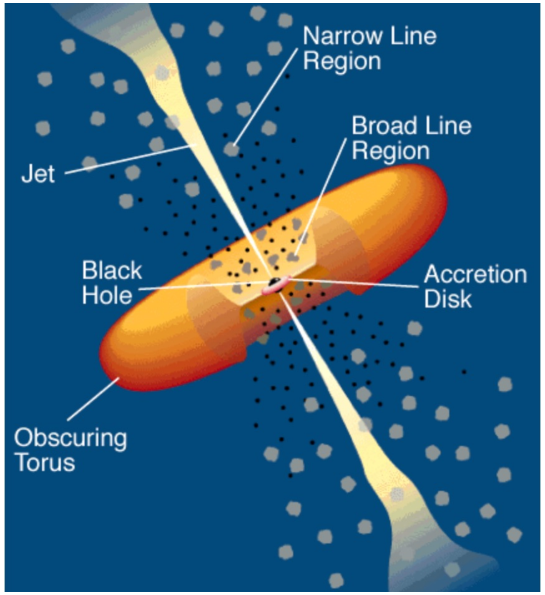

Elvis et al. (2002)

AGNs are surrounded by very dense ionized clouds ($n_{gas} \approx 10^{11}$ cm^{-3}) which emit a large number of recombination and collisionally excited lines

these clouds are located < 1 pc of the BH and move with high velocities (% c) resulting in highly Doppler broadened emission lines → Broad Line Region (BLR)

in the BLR, $T_{gas} \approx 2\ 10^4$ K, too high for dust formation

a fraction of the clouds are in outflow and as they move outward (few pc), the gas cools and there is a window (T, n) that allows dust condensation

for quasars luminosity $L_{bol} \approx 10^{46}$ erg/s, the **DPR ≈ 0.01 M_{sun}/yr**

smoking quasars

2D magneto-hydrodynamical simulation

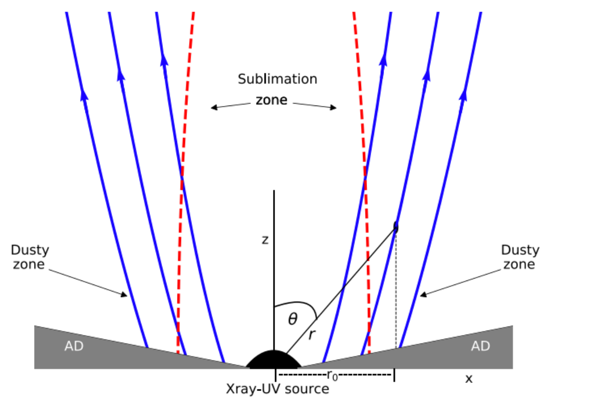

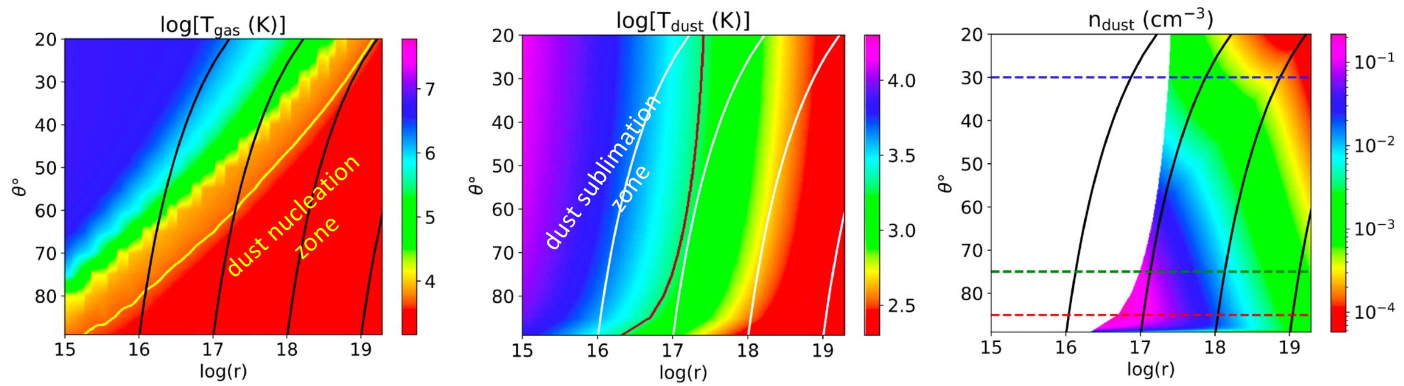

Sarangi et al. (2019)

$M_8 = M_{bh}/10^8\ M_{sun}$

upper limit for dust production: $\dot{M}_{dust} \simeq 3.5 \dot{m}^{2.25} M_8\ M_{\odot} yr^{-1}$

$dm/dt = (dm_{bh}/dt)/(dm/dt)_{Edd} \approx 0.1 - 1$

DPR < 0.01 – 3.5 M_{sun}/yr

Outline of lectures

Lecture 1

- core-collapse SN dust formation and survival
- AGB dust formation
- Type Ia SN
- Smoking quasars: dust formation in super-extreme environments

Lecture 2

- SN vs AGB stars as cosmic dust polluters
- Life after formation: dust reprocessing in the ISM
- modeling dust in galaxy evolution

SNe vs AGB stars as cosmic dust polluters

relative importance of SNe and AGB stars depends on their mass- and metallicity-dependent yields (mdust), the stellar Initial Mass Function (IMF) and the star formation history SFR(t)

total dust mass produced by stars at time t

$$M_{\rm d}(t) = \int_0^t dt' \int_{m_{\tau_m}}^{m_{\rm up}} m_{\rm dust}(m, Z)\, \phi(m)\, {\rm SFR}(t' - \tau_m)\, dm,$$

Valiante et al. (2009)

mass of a star with lifetime $\boldsymbol{\tau}_m$ formed at time t'- $\boldsymbol{\tau}_m$

SNe vs AGB stars as cosmic dust polluters: star formation history

relative importance of SNe and AGB stars depends on their mass- and metallicity-dependent yields (mdust), the stellar Initial Mass Function (IMF) and the star formation history SFR(t)

shaded regions encompass metallicity variation

no SN reverse shock

SN reverse shock

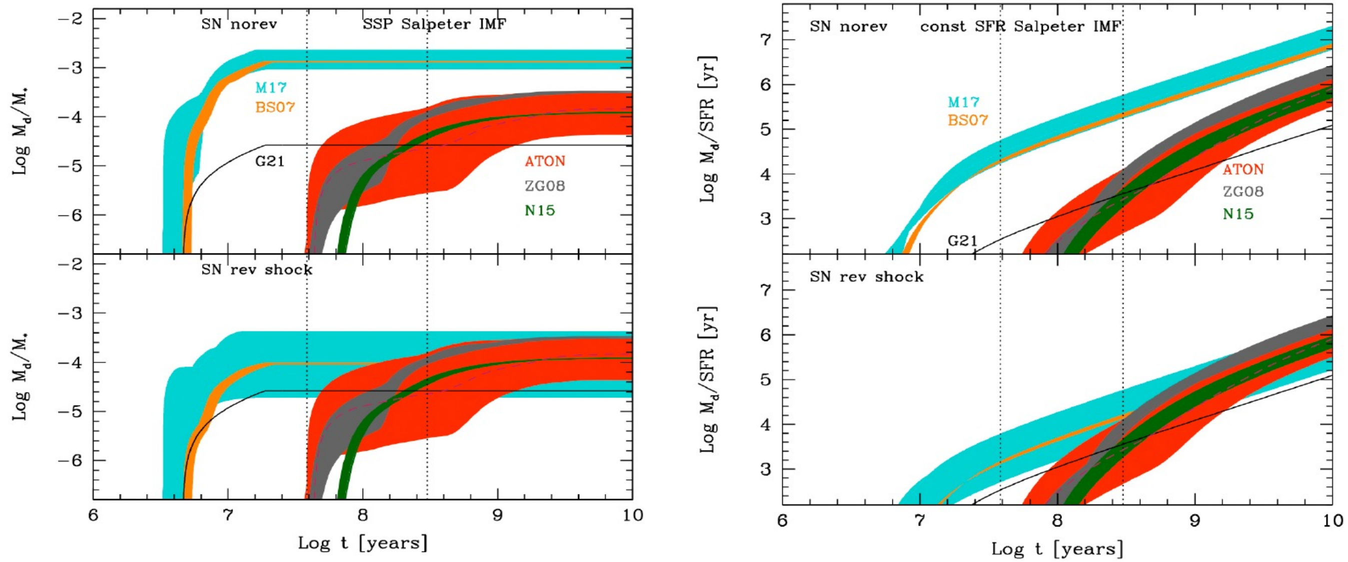

delay before SN explosions < 10 Myr

delay before massive AGB > 30 Myr

relative role depends on:

- effective SN dust yields (effects of reverse shock)
- stellar metallicity
- AGB stars dominate on t > 1 Gyr only if reverse shock destruction reduces SN dust

SNe vs AGB stars as cosmic dust polluters: stellar IMF

$\phi(m) = m^{-(\alpha+1)} e^{-m_{ch}/m}$, **α** = 1.35 m_{ch} = 0.35 M_{sun}, 5 M_{sun}, 10 M_{sun} Larson IMF

instantaneous stellar burst at t = 0

shaded regions encompass metallicity variation

m_{ch} = 0.35 M_{sun} m_{ch} = 5 M_{sun} m_{ch} = 10 M_{sun}

no SN reverse shock

SN reverse shock

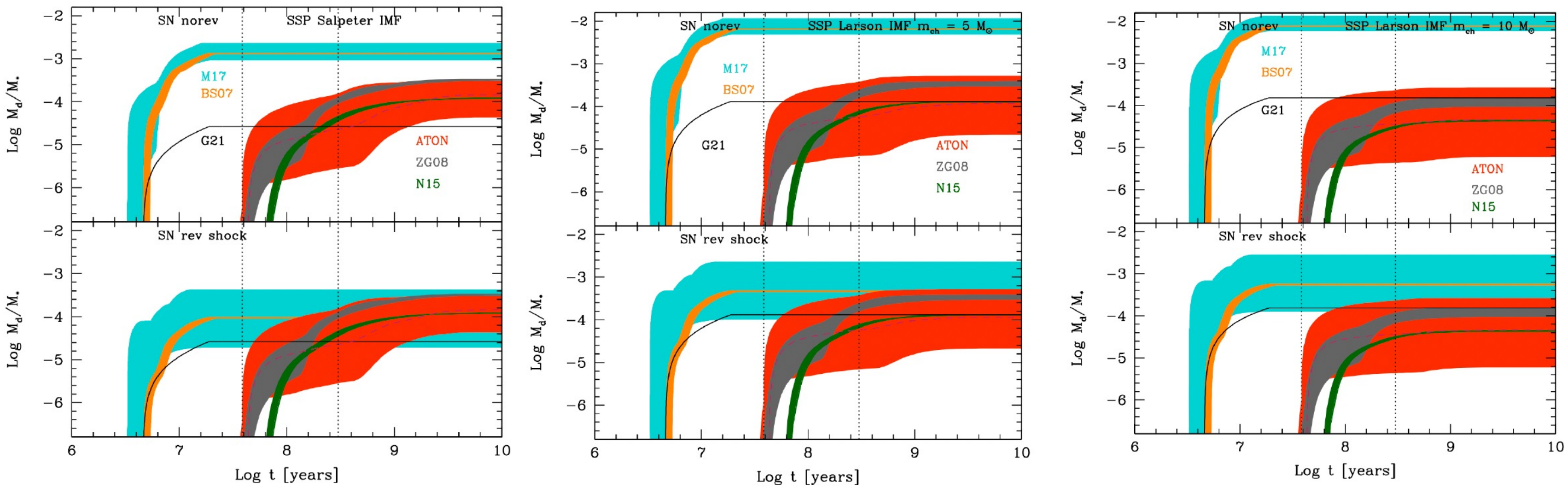

for a top-heavy stellar IMF (mch > 5 Msun) AGB stars are always subdominant even when SN dust is destroyed by the reverse shock

for the most efficient models, we can expect between $10^{-3} < M_d/M_* < 10^{-2}$ of stellar dust injected in the ISM

life after formation: dust reprocessing in the ISM

Draine (2009), Hirashita (2013), and Galliano et al. (2018) for excellent reviews

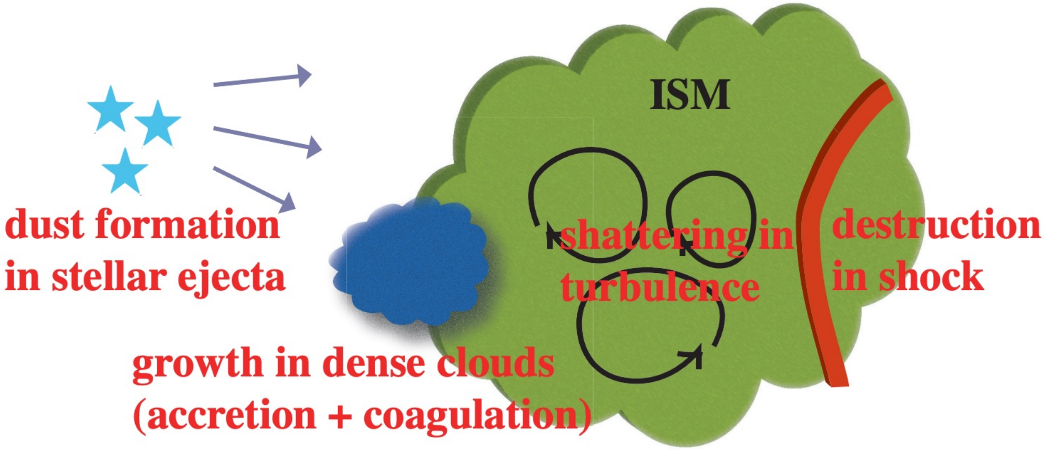

Hirashita (2013)

Category[a]	Process	Section[b]	Dust mass[c]	Extinc.[d]
	Stellar ejecta	3.1	↗	flat
(i)	Shock destruction	3.2	↘	flat
	Grain growth	3.3	↗	steep
(ii)	Shattering	4.1	⟶	steep
	Coagulation	4.2	⟶	flat

- destruction in interstellar shocks
- grain growth in the interstellar medium

dust destruction in interstellar shocks

expanding shock waves of SNe destroy pre-existing dust in the interstellar medium (Jones et al. 1996)

modification of grain size distribution assuming dust uniformly mixed in the ISM n = 0.25 cm^{-3} and shock velocity v_{sh}

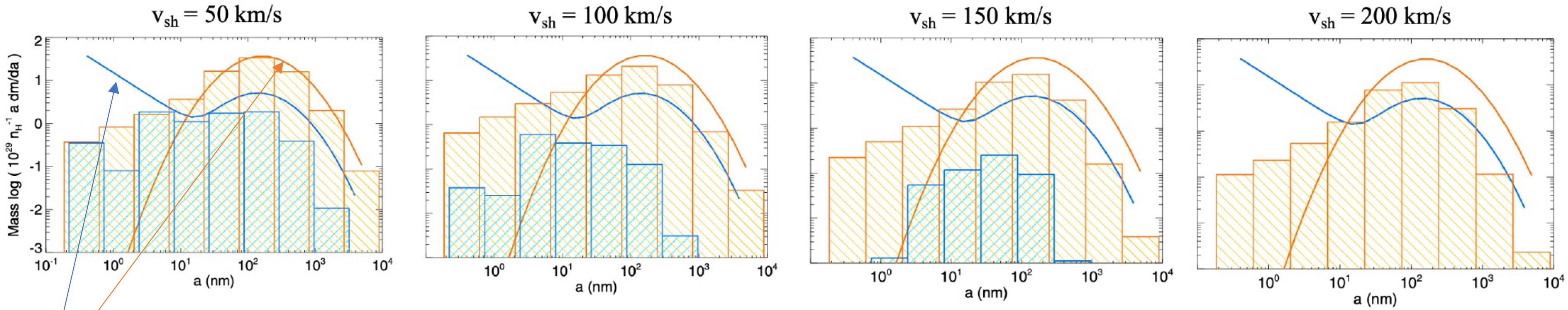

Bocchio et al. 2014

pre-shock carbon and silicate grains (Jones et al. 2013)

- carbon grains are completely destroyed when v_{sh} > 150 km/s
- silicate grains are more resistant, their size distribution is significantly affected when v > 100 km/s

dust destruction in interstellar shocks

expanding shock waves of SNe destroy pre-existing dust in the interstellar medium (Jones et al. 1996)

grain destruction efficiencies assuming dust uniformly mixed in the ISM n = 0.25 cm^{-3} and shock velocity $v_{s7} = v_{sh}/(100 km/s)$

$$\epsilon_{carb}(v_{s7}) = \begin{cases} 0.66 + 0.23\, v_{s7} & \text{for} \quad 0.5 < v_{s7} \leq 1.5 \\ 1 & \text{for} \quad 1.5 < v_{s7} \leq 2 \end{cases}$$

$$\epsilon_{sil}(v_{s7}) = \begin{cases} 0.61\, v_{s7} - 0.31 & \text{for} \quad 0.5 < v_{s7} \leq 1.25 \\ 0.11 + 0.28\, v_{s7} & \text{for} \quad 1.25 < v_{s7} \leq 2 \end{cases}$$

Bocchio et al. 2014

→ for $v_{s7} = 1$ $\varepsilon_{carb} = 0.89$ and $\varepsilon_{sil} = 0.30$

significant smaller fraction in small grains

the results depend on the adopted initial size distribution:

for MRN size $dN/da \approx a^{-3.5}$ 5 nm < a < 250 nm Slavin et al. (2015) find $\varepsilon_{carb} = 0.10$ and $\varepsilon_{sil} = 0.23$

dust destruction in interstellar shocks

dust destruction efficiencies can be used to evaluate the dust destruction timescale, $\boldsymbol{\tau}_{dest}$, also known as the lifetime of dust against destruction by SN shocks (Dwek & Scalo,1980):

$$\frac{1}{\tau_{\rm dest}} = \frac{R_{\rm SN}\, m_{\rm gas}^{\rm dest}}{M_{\rm ISM}}$$

M_{ism} = mass of ISM material
R_{SN} = rate of SN explosions
m_{gas}^{dest} = mass of ISM completely cleared out of dust by a single SN explosion

$$m_{\rm gas}^{\rm dest} = \int \epsilon(v_{\rm s})\, dM_{\rm s}(v_{\rm s}),$$

$M_s(v_s)$ is the mass of ISM shocked to a velocity of v_s

$E_{51} = E_{SN}/10^{51}$ erg

$$M_{\rm s}(v_{\rm s}) = \frac{E_{\rm SN}}{\sigma v_{\rm s}^2} = 6800\, M_\odot \frac{E_{51}}{v_{\rm s7}^2},$$

for a Sedov-Taylor blastwave expanding in a uniform medium (McKee, 1989)

$\boldsymbol{\sigma}$ = 0.89

results of different studies, particularly those based on hydro-dynamical simulations, are compared in terms of m_{gas}^{dest}

comparing SN shocks dust destruction efficiencies

dust destruction efficiencies by a single SN explosion in a homogeneous medium

Reference	carb $m_{\mathrm{gas}}^{\mathrm{dest}}[M_{\odot}]$	sil $m_{\mathrm{gas}}^{\mathrm{dest}}[M_{\odot}]$	Notes
Bocchio et al. (2014)	21100	4220	$n_{\mathrm{ISM}} = 0.25\ \mathrm{cm}^{-3}$, $E_{51} = 1$
Slavin et al. (2015)	1220	1990	$n_{\mathrm{ISM}} = 0.25\ \mathrm{cm}^{-3}$, $E_{51} = 1$
Hu et al. (2019)	1330 (1050)	1990 (1370)	$n_{\mathrm{ISM}} = 0.1\ (1)\ \mathrm{cm}^{-3}$, $E_{51} = 1$
Kirchschlager et al. (2022)	–	6470 (7090)	$n_{\mathrm{ISM}} = 0.1\ (1)\ \mathrm{cm}^{-3}$, $E_{51} = 1$
	dust mix $m_{\mathrm{gas}}^{\mathrm{dest}}[M_{\odot}]$		
Martínez-González et al. (2019)	~ 45	WDB	$n_{\mathrm{ISM}} = 1\ \mathrm{cm}^{-3}$, $E_{51} = 0.9$
Martínez-González et al. (2019)	> 120	no WDB	$n_{\mathrm{ISM}} = 1\ \mathrm{cm}^{-3}$, $E_{51} = 0.9$

evaluated at t ≈ 10^3 kyr

explosion within a pre-exisitng wind driven bubble

multiphase ISM

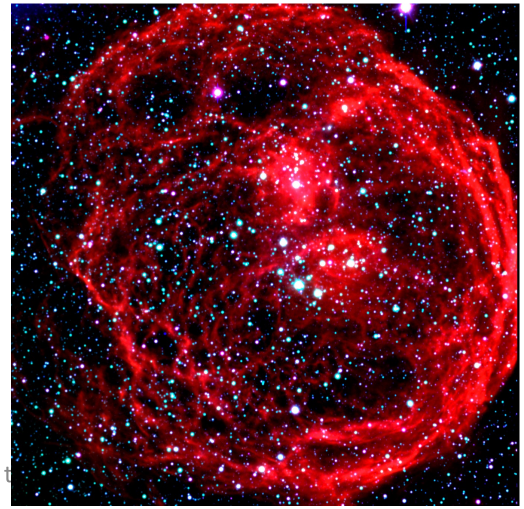

temporal/spatial correlations among SNe

effective SN shock dust destruction

$$\frac{1}{\tau_{\rm dest}} = \frac{R_{\rm SN,eff}\, m^{\rm dest}_{\rm gas,eff}}{M_{\rm ISM}}$$

$$R_{\rm SN,eff} = \delta_{\rm SN} R_{\rm SN}$$

$$m^{\rm gas,eff}_{\rm dest} = f_{\rm eff}\, m^{\rm dest}_{\rm gas}$$

from observations in the Milky Way $\boldsymbol{\delta}_{SN} \approx 0.36$ (McKee 1989) and 3D simulations $\boldsymbol{\delta}_{SN} \approx 0.40$ (Hu et al. 2019)

in a 3-phase ISM the volume filling factors of cold, warm, hot phases are: $f_c \approx 0.02$, $f_w \approx 0.3$, $f_h \approx 0.7$

dust destruction mosly occurs in the warm phase (hot phase is too tenuous, cold phase has too small f_c) hence:

$f_{eff} = f_w/f_h \approx 0.43$ (McKee 1989)

if the galaxy is dominated by the warm phase: $f_{eff} = f_w \approx 0.8$ (Slavin et al. 2015)

comparing dust lifetimes against SN destruction in the MW

$$\frac{1}{\tau_{\rm dest}} = \frac{R_{\rm SN,eff}\, m^{\rm dest}_{\rm gas,eff}}{M_{\rm ISM}}$$

$$M_{\rm ISM} = 4.5 \times 10^9\, M_\odot$$

$$R_{\rm SN,eff} = 1/125\ {\rm yr}^{-1}$$

f_{eff} = 0.43 – 0.8

$m^{\rm dest}_{\rm gas}$ from different studies

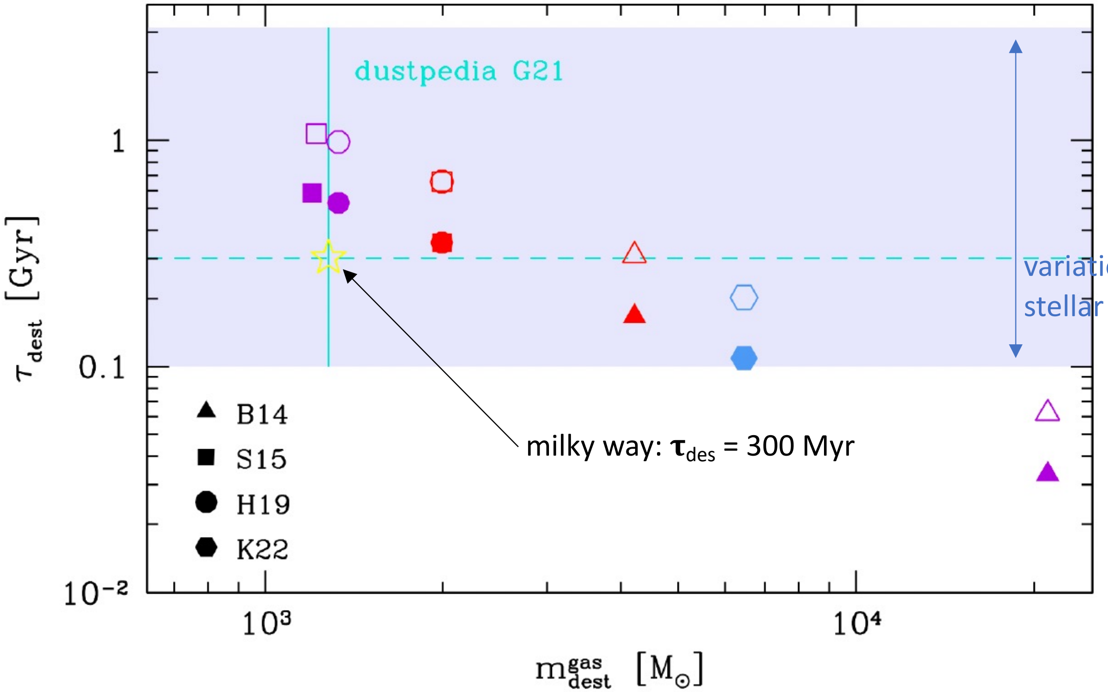

empty symbols f_{eff} = 0.43

filled symbols f_{eff} = 0.80

carbon grains

silicate grains

variation among different galaxies spanning a broad range of SFHs, metallicities, stellar masses, SFRs…

f_{eff}, δ_{SN} are non-universal but depend on the physical conditions of the ISM

grain growth in the ISM

Why do we need grain growth in the ISM?

Draine (2011):

mean residence time of an atom in the ISM of the Milky Way is $\boldsymbol{\tau}_{SF} = M_{ISM}/SFR \approx 4.5\ 10^9\ M_{sun}/(\approx 5\ M_{sun}/yr) = 10^9$ yr

if we assume all Si atoms enter the ISM as stardust grains, only a fraction $\boldsymbol{\tau}_{dest}/(\boldsymbol{\tau}_{dest}+\boldsymbol{\tau}_{SF}) \approx 0.3/(0.3+1) \approx 0.23$ would still be in the ISM today

observations show that ≈ 90% of Si atoms are depleted onto dust grains (Jenkins 2009)

→ most of currently observed Si grains must form in the ISM (Draine 2011)

empirical evidences for grain growth in the ISM

- variations in grain emissivity that could be explained by grain coagulation and growth (Kohler+2015; Ysard+2015);
- correlation of depletion factor with density (Jenkins, 2009; Tchernyshyov+2015; Jenkins & Wallerstein, 2017; Roman-Duval+2021)

resolved FIR observations + atomic/molecular gas maps indicate dust-to-gas-mass ratio (DtG) that increases with density as predicted by grain growth (Roman-Duval et al., 2017; Clark et al., 2023)

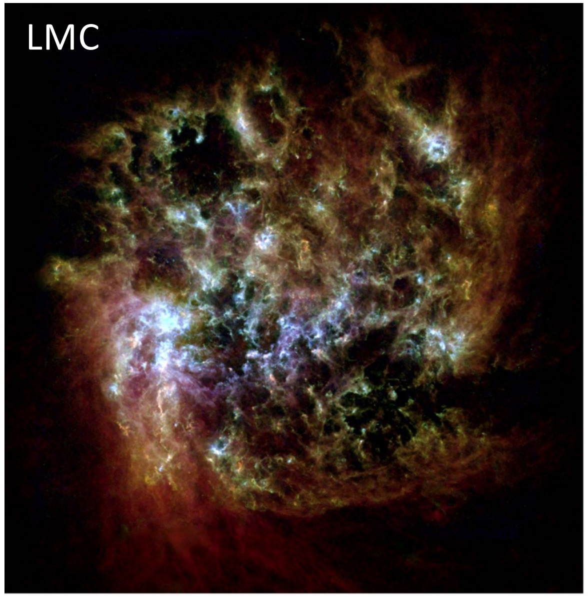

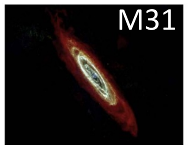

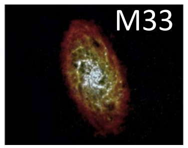

Red: H gas
(21 cm and CO emission)
Green: Herschel-SPIRE 350 µm
cooler dust emission
Blue: Herschel-PACS 100 µm
warmer dust emission

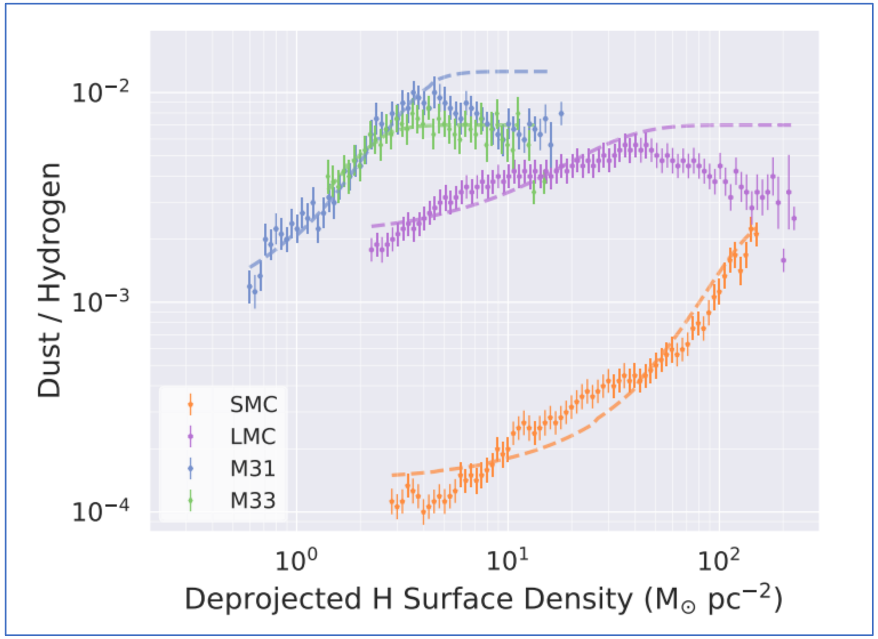

Clark+(2023)

empirical evidences for grain growth in the ISM

the relation between the D/G and metallicity in local galaxies does not follow a linear trend, but shows a knee, at approximately $Z \approx 0.2\ Z_{sun}$, below which the D/G drops sharply (Remy-Ruyer+2014; Galliano+2018; De Vis+2019; Galliano +2021).

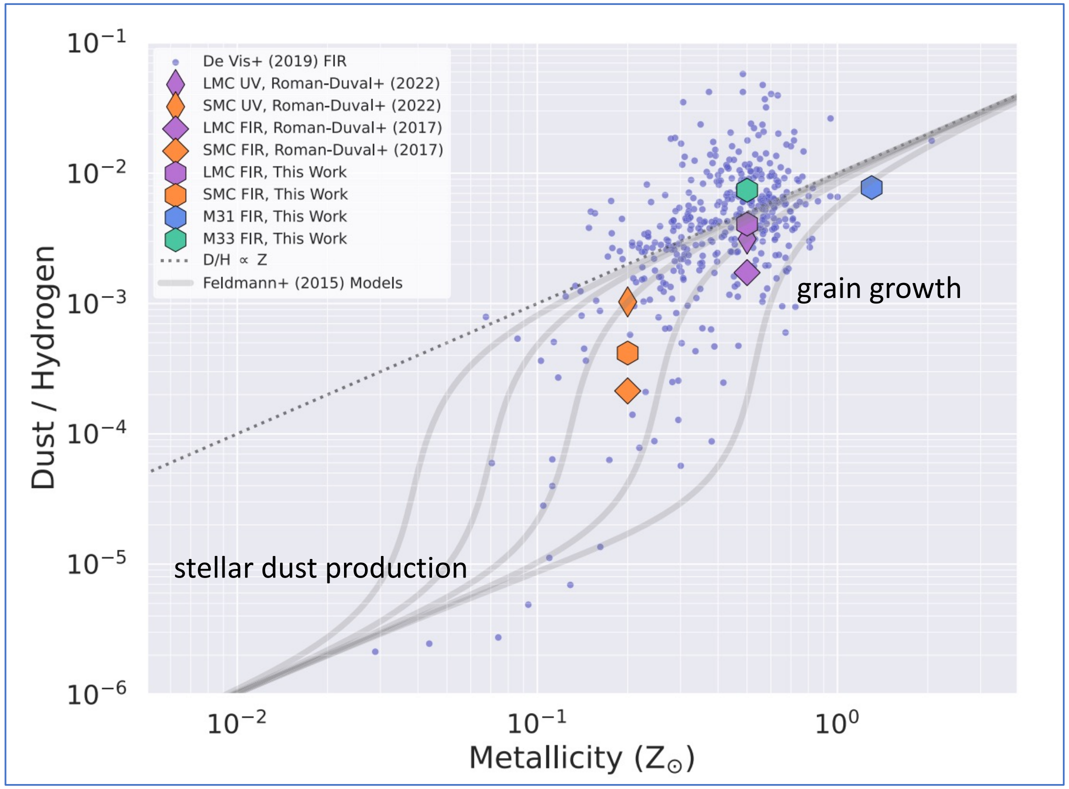

Clark+2023

grain growth in the ISM

we do not yet understand how grains can growth in the ISM

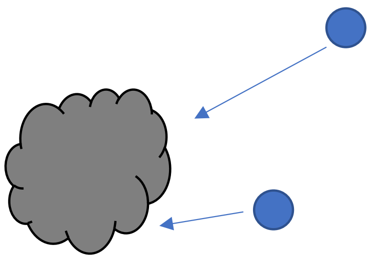

1) Kinetics

the collision rate between ions and grains depends on the n, T of the ISM, on the geometrical cross section of the grains, and on the grain charge (neutral, negatively charges grains have increased collision rate with positively charged ions due to Coulomb focusing)

number density of ions

in the CNM (n ≈ 30 cm^{-3} T ≈ 100 K) the accretion timescale: $\tau_a^{-1} = -\frac{1}{n}\frac{dn}{dt},$

is ≈ 15 Myr for Si and Fe grains and can be reduced to ≈ 0.1 – 1 Myr with Coulomb focusing

Weingartner & Draine (1999, Draine (2009); Zhukovska (2014)

grain growth in the ISM

we do not yet understand how grains can growth in the ISM

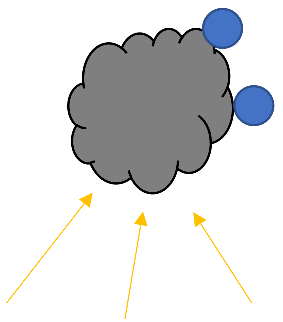

2) Surface reactions

the colliding atom or ion must also be bound to the surface of the grain in a way that it allows it to be retained against thermal desorption, UV and Cosmic Ray irradiation

see Draine (2009), Zhukovska et al. (2016), Ferrara et al. (2016), and Ceccarelli et al. (2018).

the accreted species need to find an «active» site on the surface before being thermally desorbed:

scanning timescale < thermal desorption timescale ($\tau_s < \tau_{d,th}$)

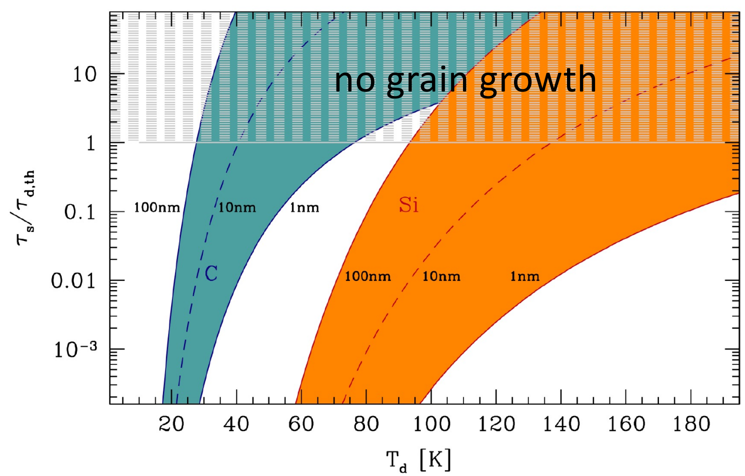

dust temperature

- for small grains there is a range of grain temperature for which $\tau_s < \tau_{d,th}$
- τ_s < 1 Myr when T_d > 25 - 30 K (> 10 K) for for Si (C) atoms scanning grains with a < 100 nm

grain growth in the ISM

we do not yet understand how grains can growth in the ISM

1) Kinetics

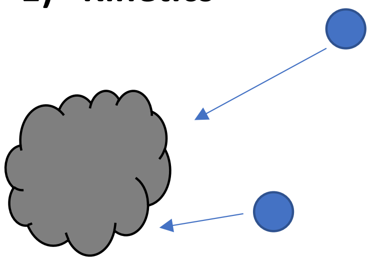

2) Surface reactions

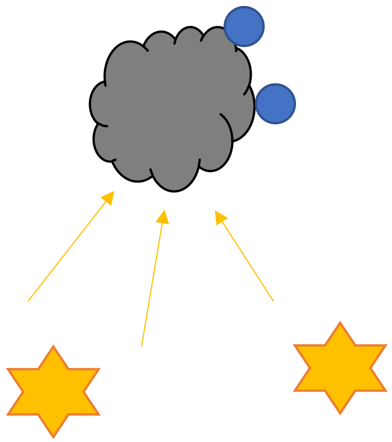

very small grains, with sizes ≈ 10 – 100 nm
are likely to be critical for grain growth in the CNM
as they have:

- the largest total surface area
- the highest fraction of negatively charged grains
- aided by stochastic heating, their $\tau_s < \tau_{d,th}$

grain growth in the ISM

chemical evolution models generally adopt a simplified description of the process (Asano+2013, Mattsson & Andersen 2012)

dust mass growth rate:

$$\left(\frac{dM_d}{dt}\right)_{growth} = N_d \, \pi < a^2 > S \, \rho_Z^{gas} < v >,$$

S: sticking coefficient
ρ_{Zgas} density of gas phase metals
<v>: mean velocity of gas-phase metals

number of grains: $N_d = M_d/m_d$
mass of an individual grain: $m_d = 4/3 \, \pi <a^3> \sigma$

grain growth timescale:

$<a^3>/<a^2>$

$$\tau_{growth} = M_d \left(\frac{dM_d}{dt}\right)^{-1}_{growth} = 6.7 \times 10^6 \, yr \left(\frac{\bar{a}}{10\,nm}\right)\left(\frac{n_H}{30\,cm^{-3}}\right)^{-1}\left(\frac{T}{100\,K}\right)^{-1/2}\left(\frac{Z}{Z_\odot}\right)^{-1}$$

for the CNM this leads to $\tau_{growth} \approx 6.7$ Myr for 10 nm characteristic size and solar metallicity

in local galaxies τ_{growth} spans a broad range of values, from ≈ 1 Gyr for the lowest metallicity systems to ≈ 45 Myr for $Z \approx Z_{sun}$
implying that grain growth occurs for a broader range of grain sizes and ISM conditions

dust in the Milky Way and local galaxies

chemical enrichment in a cosmological context

GAMESH: semi-analytical galaxy formation model +
dark matter simulation coupled to the radiative transfer code CRASH Graziani+2014, 2015

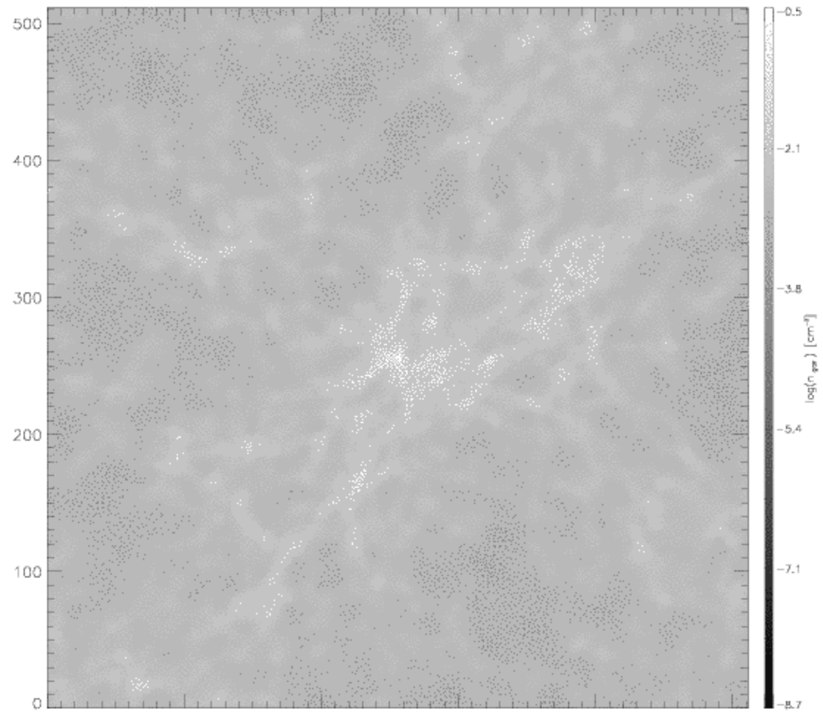

Dark matter simulation of the Milky Way galaxy in Planck cosmology GCD+ code with multi-resolution technique (Kawata & Gibson 2003):

Low-res spherical region of R_l ~ 20 h^{-1} Mpc taken from a low-res cosmological simulation

High-res spherical region of R_h ~ 2 h^{-1} Mpc with M_p = 3.4 x 10^5 M_{sun}

where does Galactic dust come from?

stellar dust production along the build-up of the MW

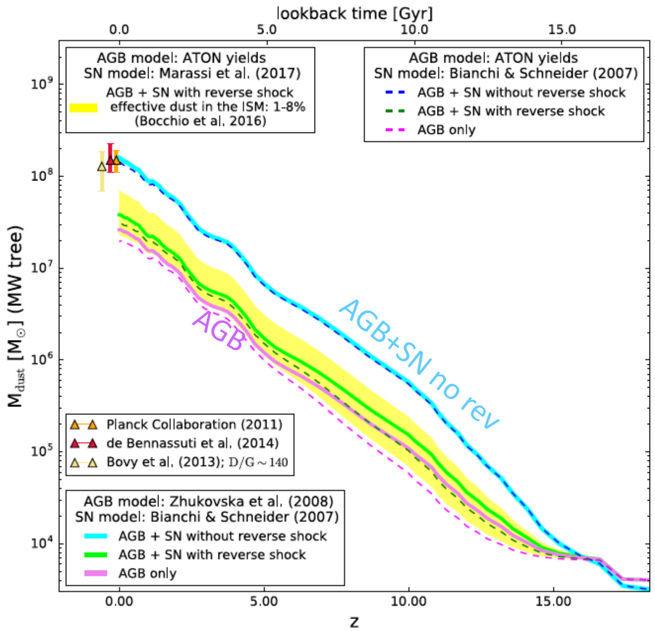

dust-to-gas mass ratio vs metallicity: stellar dust sources

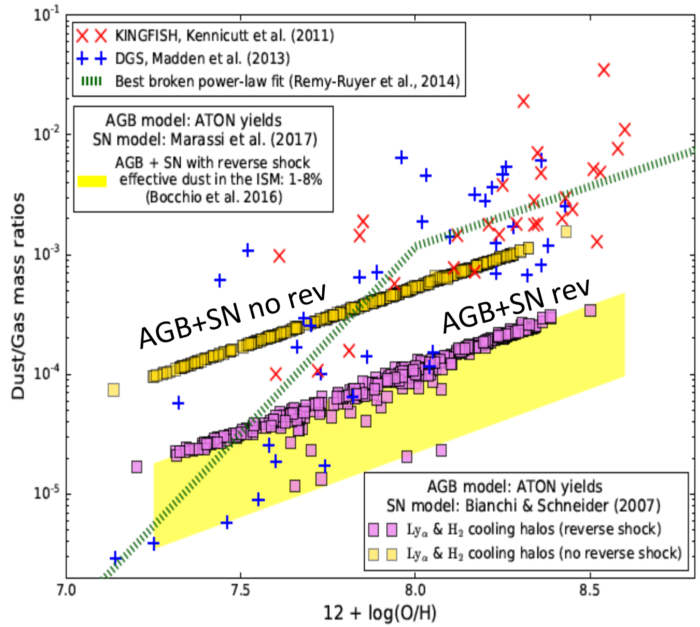

Ginolfi, Graziani, RS et al. 2018

- the injected and surviving dust mass is a factor 4-5 smaller than observed in the MW (unless no reverse shock)
- models with stellar dust only can not reproduce the observed scaling relations between the dust-to-gas mass and Z

these conclusions are independent of the adopted dust yields

Remy-Ruyer et al. 2014; Asano+2013; Zhukovska+2014; Schneider+14; Feldman+15; Popping+16, Galliano+18

chemical evolution with dust

$$\frac{dM_*(t)}{dt} = \mathrm{SFR}(t) - \frac{dR(t)}{dt},$$

stellar mass

$$\frac{dM_{\mathrm{ISM}}(t)}{dt} = -\mathrm{SFR}(t) + \frac{dR(t)}{dt} + \frac{dM_{inf}(t)}{dt} - \frac{dM_{ej}(t)}{dt} - (1-\epsilon_r)\frac{dM_{accr}(t)}{dt}$$

gas mass

$$\frac{dM_Z(t)}{dt} = -Z_{\mathrm{ISM}}(t)\mathrm{SFR}(t) + \frac{dY_Z(t)}{dt} + Z_{\mathrm{vir}}(t)\frac{dM_{inf}(t)}{dt} - Z_{ISM}(t)\frac{dM_{ej}(t)}{dt} - Z_{\mathrm{ISM}}(t)(1-\epsilon_r)\frac{dM_{accr}(t)}{dt}$$

metal mass

$$\frac{dM_d(t)}{dt} = -Z_d(t)\mathrm{SFR}(t) + \frac{dY_d(t)}{dt} - \frac{M_d^{diff}(t)}{\tau_d} + \frac{M_d^{mc}(t)}{\tau_{acc}} - Z_d(t)(1-\epsilon_r)\frac{dM_{accr}}{dt}$$

$$\tau_{\mathrm{acc}} \approx 20\,\mathrm{Myr} \times \left(\frac{\bar{\mathrm{a}}}{0.1\,\mu\mathrm{m}}\right)\left(\frac{\mathrm{n}}{100\,\mathrm{cm}^{-3}}\right)^{-1}\left(\frac{\mathrm{T}}{50\,\mathrm{K}}\right)^{-1/2}\left(\frac{\mathrm{Z}}{\mathrm{Z}_\odot}\right)^{-1}$$

$$\tau_d = \frac{M_{\mathrm{ISM}}(t)}{\epsilon_d M_{swept} R'_{\mathrm{SN}}},$$

dust mass

the lifecycle of dust in the Milky Way

——— average over 50 independent merger trees

▇ 1 – σ

de Bennassuti et al 2014

global properties of the MW | 2-phase structure of the ISM | Pop III and Pop II SFRs

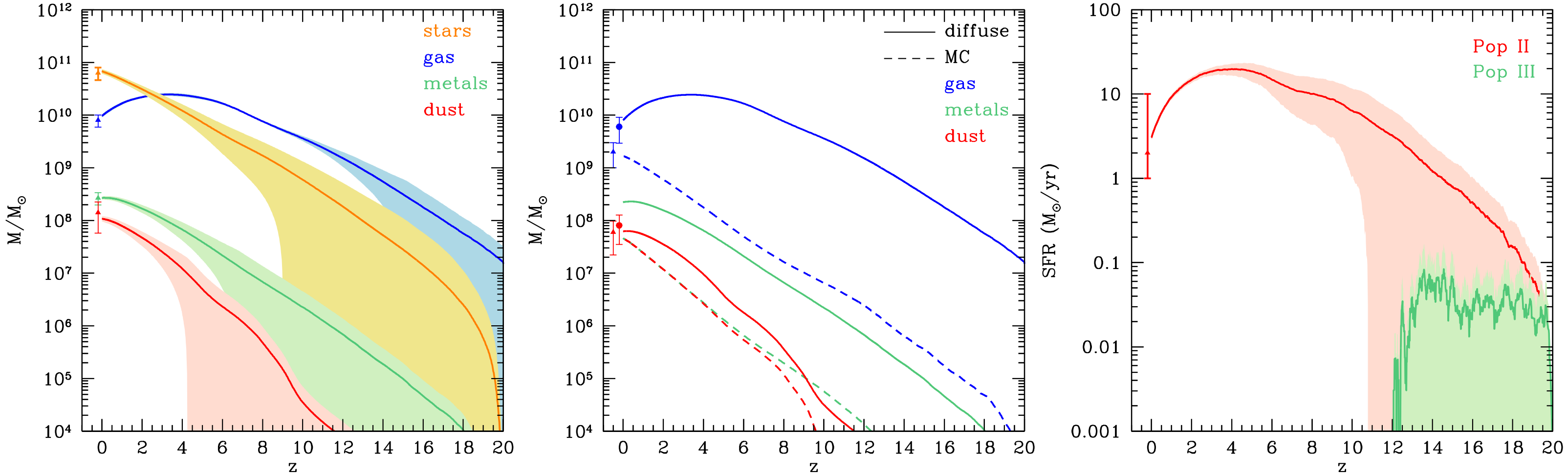

the existing dust mass is well reproduced and the predicted depletion factors are 1 for the MC phase and 0.3 for the diffuse phase → consistent with observed depletion (Jenkins 2009)

the MW and its dusty progenitors

de Bennassuti et al 2014

dust-to-gas ratio versus metallicity

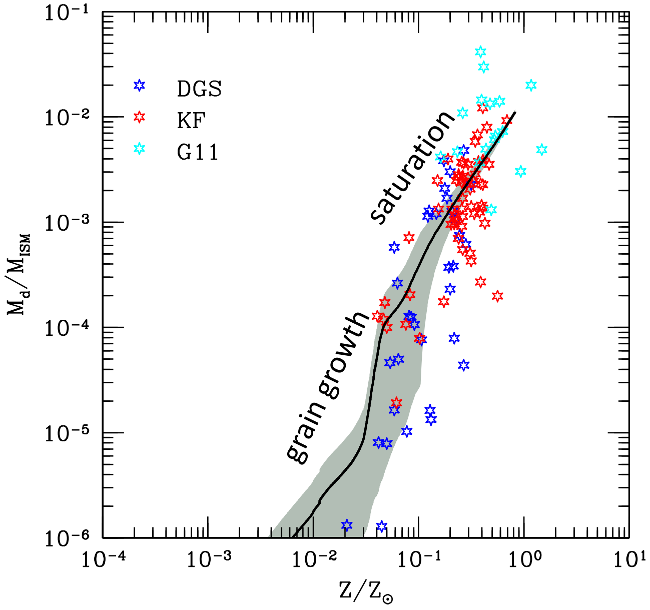

data points:
Local dwarfs Galametz et al. (2011)
Madden et al. (2013),
Remy-Ruyer et al. (2014)

dust mass evolution

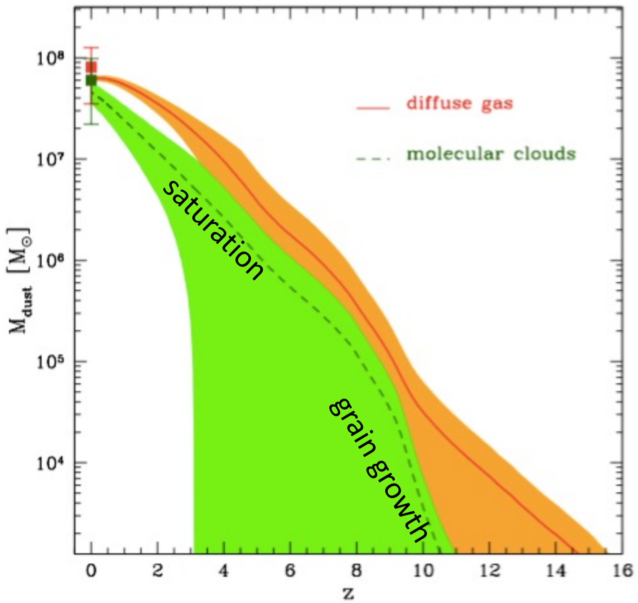

grain growth provides the dominant contribution to the existing dust mass in the MW

the dust mass depends on ISM conditions

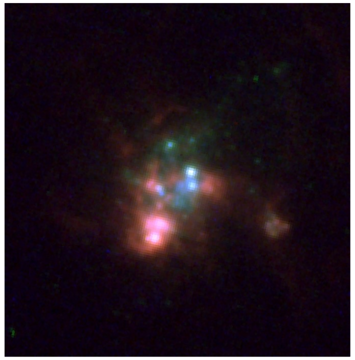

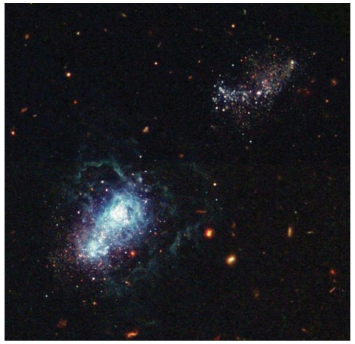

dust-to-gas ratio vs metallicity

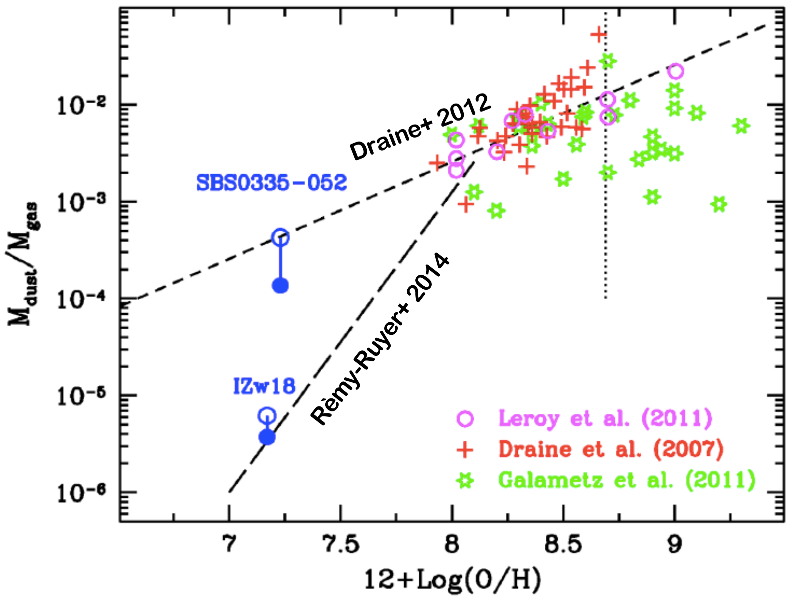

RS, Hunt & Valiante 2016

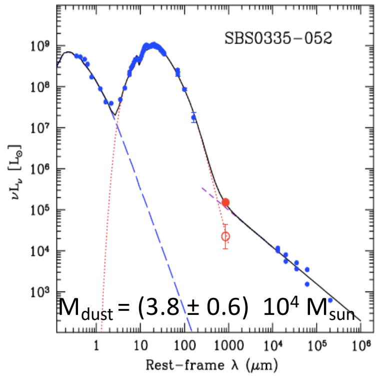

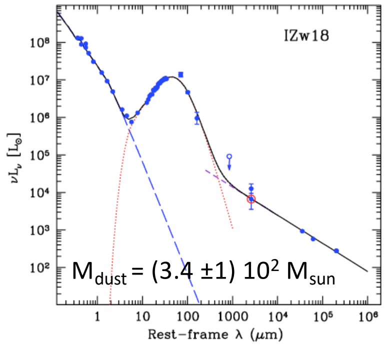

Galaxy	M_{dust}/M_{sun}	Z/Z_{sun}	n/cm^3	T/K
SBS0335-052	**3.8 x 10^4**	0.038	**1500**	80
IZw18	**340**	0.031	**100**	10

the dust mass depends on ISM conditions

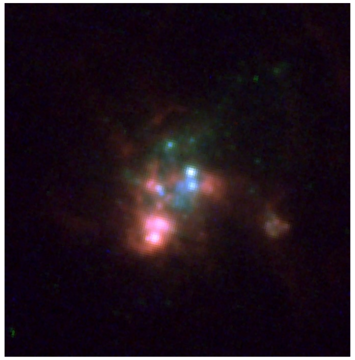

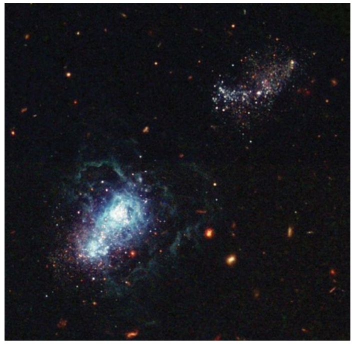

dust-to-gas ratio vs metallicity

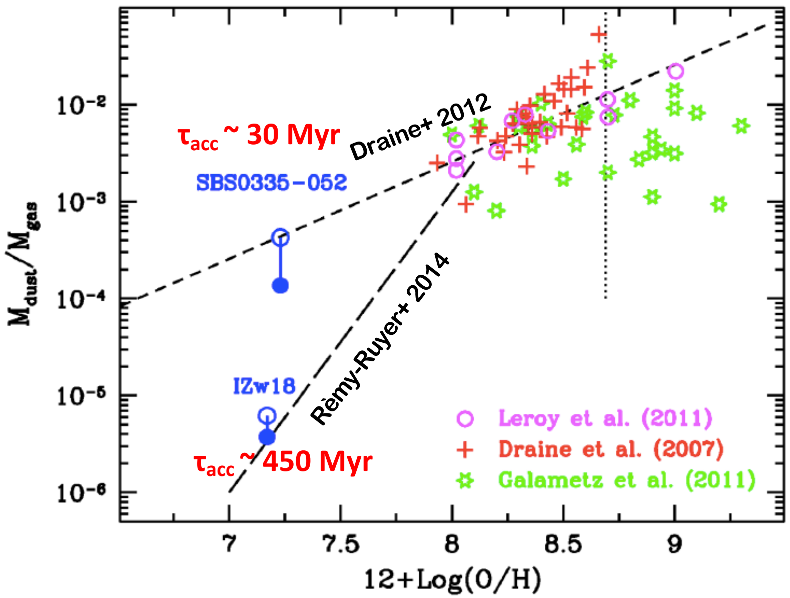

RS, Hunt & Valiante 2016

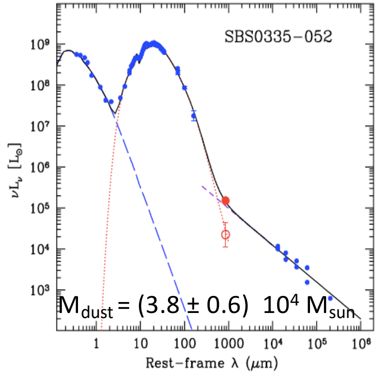

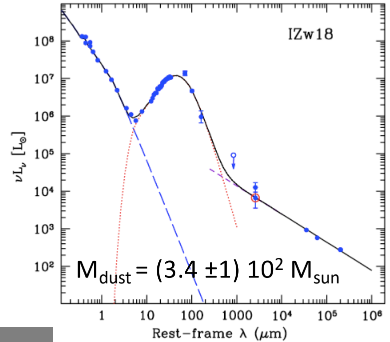

the difference in the observed dust masses could be due to different grain growth times scales

Asano+2013; Hirashita+2014

$$\tau_{acc} = \tau_{acc,0} \left(\frac{Z}{Z_{sun}}\right)^{-1} \qquad \tau_{acc,0} = 2\ \mathrm{Myr} \left(\frac{<a>}{0.1\mu m}\right) \left(\frac{n}{1000 cm^{-3}}\right)^{-1} \left(\frac{T}{50\ K}\right)^{-1/2}$$

dust in the first galaxies

the spectral energy distribution of a dusty star forming galaxy

Arp 220: a proto-typical Ultra Luminous Infrared Galaxy (ULIRG)

HST image

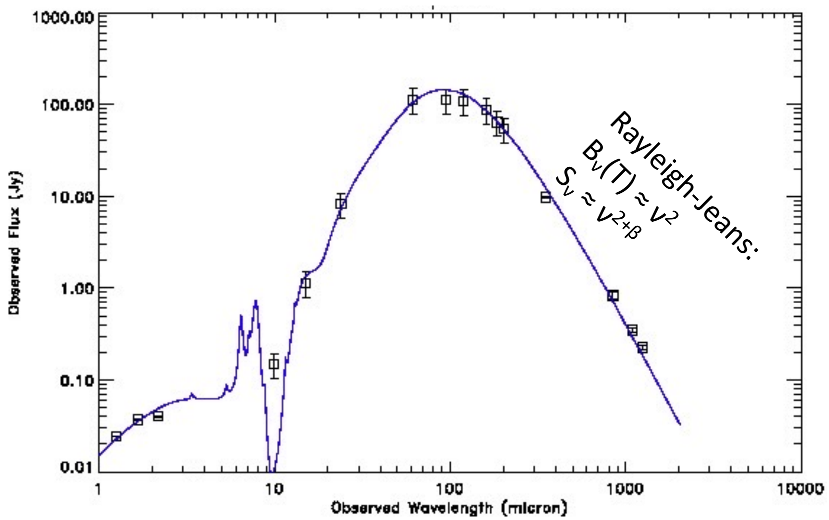

$S_\nu \approx (1 - e^{-\tau(\nu)}) B_\nu(T_{dust})/4\pi D_L^2(z)$ where $\tau(\nu) = k_\nu \, \Sigma_{dust}$ and $k_\nu = k_0 \, (\nu/\nu_0)^\beta$

at rest-frame FIR wavelengths: optically thin emission $\tau(\nu) << 1$:

$S_\nu \approx k_\nu \, B_\nu(T_{dust})/4\pi D_L^2(z)$ ←→ single temperature modified black body approximation

inferring dust masses from rest-frame FIR flux

$$M_{\rm dust} = \frac{S_{\nu_0}\, d_L^2(z)}{(1+z)\,\kappa_d(\nu)\, B(\nu, T_d)}$$

$$L_{\rm FIR} = 4\pi M_{\rm dust} \int \kappa_d(\nu)\, B(\nu, T_d)\, d\nu$$

Ref.	κ_0 [cm^2/gr]	λ_0 [μm]	β
a	7.5	230	1.5
b	30	125	2.0
c	0.4	1200	1.6
d	34.7	100	2.2
e	40	100	1.4

z = 6.4 QSO SDSS J1148

T_d [K]	$M_{\rm dust}$ [$M_\odot$]	$L_{\rm FIR}$ [$L_\odot$]
58	3.16×10^8	2.32×10^{13}
49	2.91×10^8	2.09×10^{13}
56	4.29×10^8	2.27×10^{13}
47	4.78×10^8	2.02×10^{13}
60	1.86×10^8	2.38×10^{13}

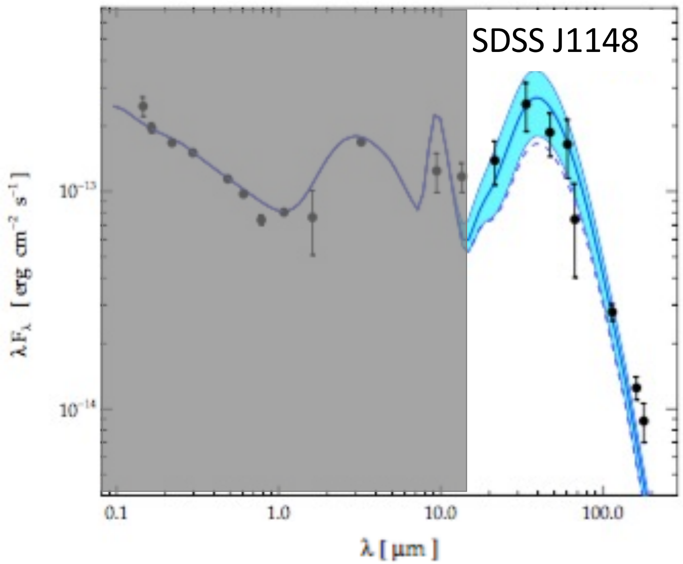

observed dust masses are uncertain

with one/two data-points there is a strong degeneracy between dust temperature and emissivity

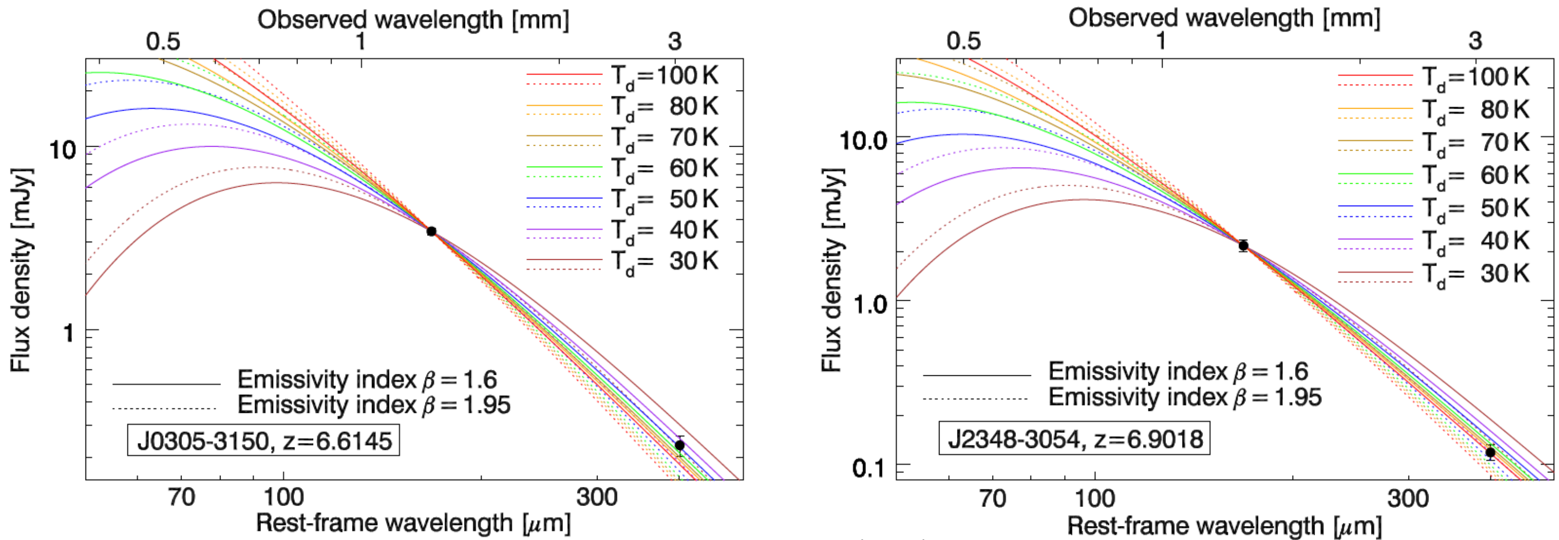

Venemans et al. (2017)

single temperature component fits

quasar	T_d	β	M_{dust}
J0305 (z=6.6)	[28 – 47]K	1.6 – 1.95	[4.5 – 24] 10^8 M_{sun}
J2348 (z= 6.9)	[40 – 94]K	1.6 – 1.95	[2.7 – 15] 10^8 M_{sun}

observed dust masses are uncertain

with one/two data-points there is a strong degeneracy between dust temperature and emissivity

ALMA observations of MACS0416_Y1 (z=8.3)

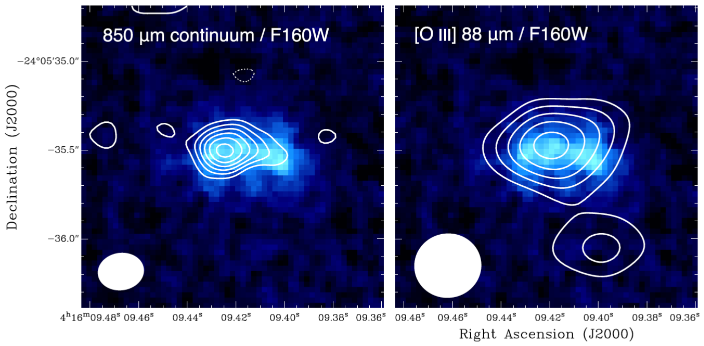

Tamura et al. (2019)

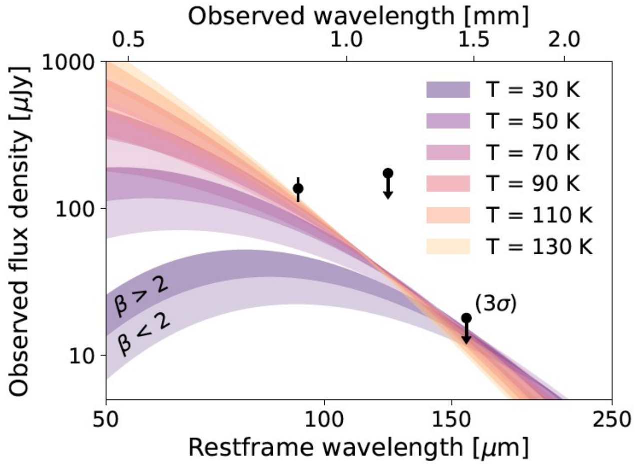

Bakx et al. (2020)

single temperature component fits

LBG - MACS0416_Y1 (z=8.3)	$\mathbf{T_d}$	**β**	$\mathbf{M_{dust}}$
Tamura et al (2019)	[40 – 50]K	1.5	[3.6 – 8.2] 10^6 M_{sun}
Bakx et al. (2020)	[60 – 121]K	1.5 – 2.5	[2.5 – 5.2] 10^5 M_{sun}

the dust mass in "extreme" galaxies at z ≈ 6: dusty SF galaxies and quasar hosts

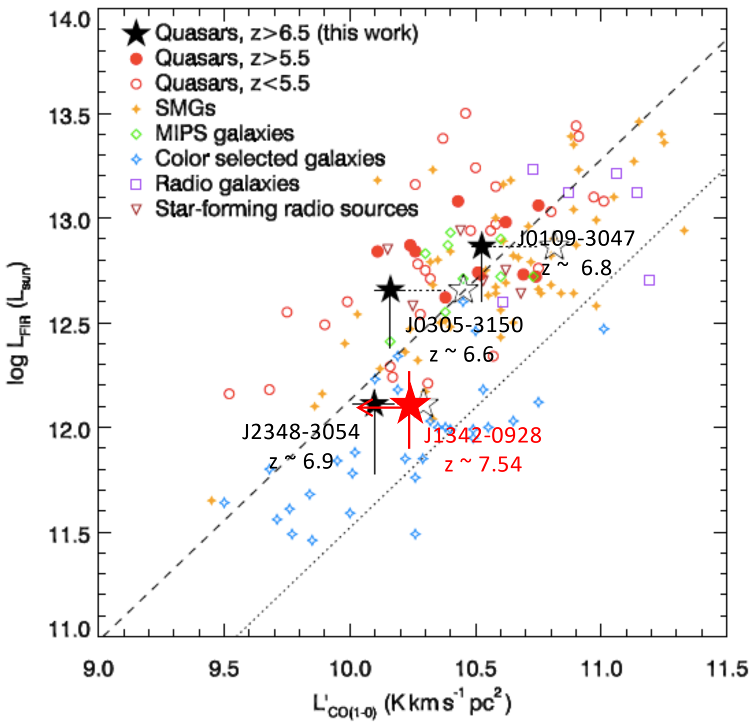

Venemans et al. 2017a,b

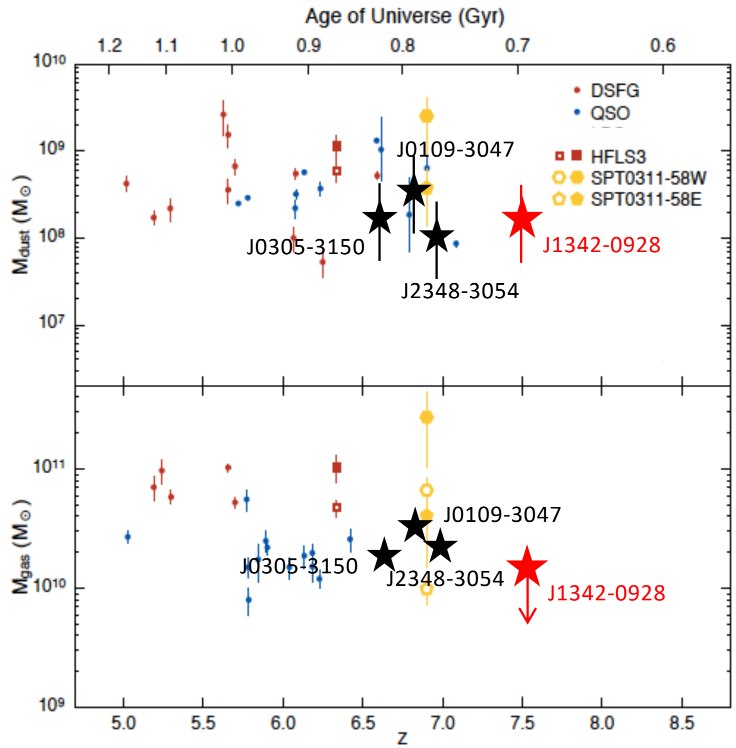

Marrone et al. 2017

Valiante et al. 2014, 2015

the dust mass in “extreme” galaxies at z ≈ 6: quasar hosts

are stellar sources enough to produce ~ 10^8 M_{sun} of dust in < 1 Gyr?

Valiante et al. 2009, 2011, 2014; Gall et al. 2010, 2011; Dwek & Cherchneff 2011; Mattsson 2011; Pipino et al 2011; Calura et al. 2013

M_{dust} *does not* correlate with M_{star}

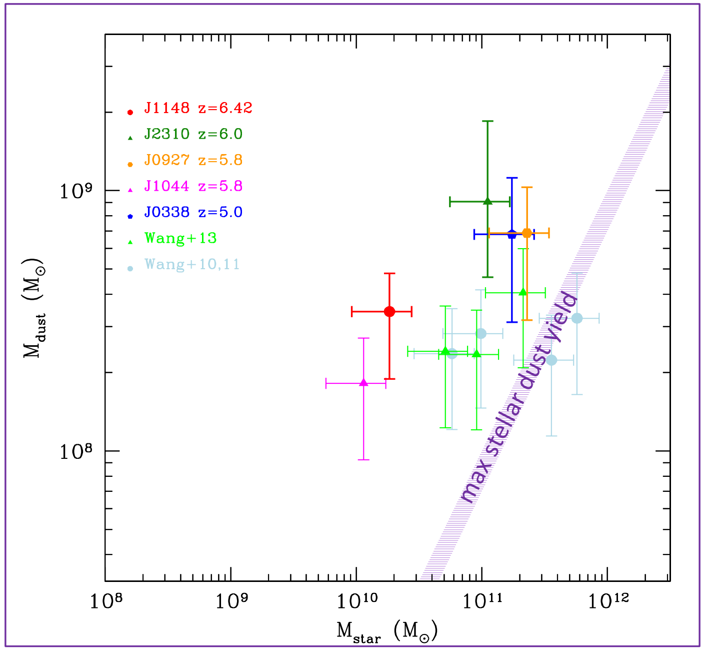

stellar dust is not enough to reproduce the observed M_{dust}

M_{dust} *does* correlate with M_{H2}

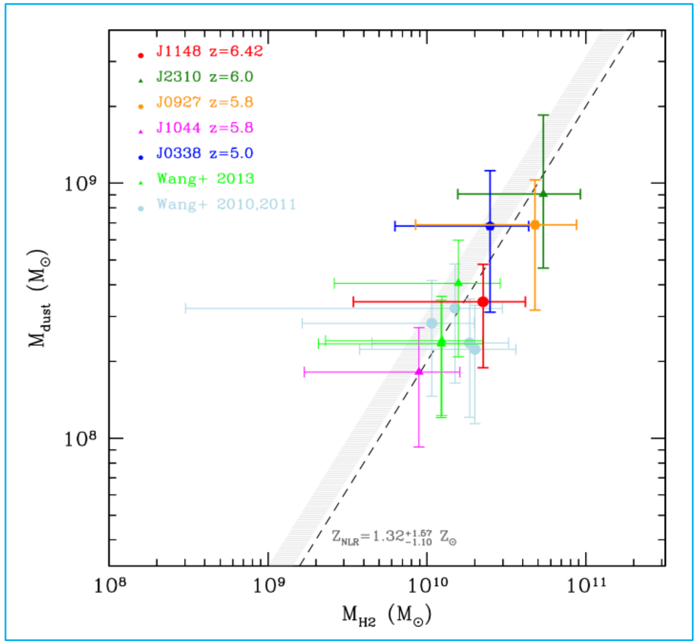

the observed M_{dust} require super-solar metallicities and very efficient grain growth in dense gas

Valiante et al. 2014, 2015

dust content of z > 7 normal star forming galaxies

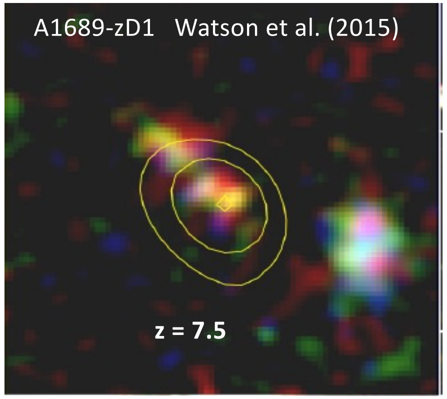

M_{star} ~ 2 10^9 M_{sun} SFR ~ 10 M_{sun}/yr
M_{dust} ~ (3 – 6) 10^7 M_{sun}

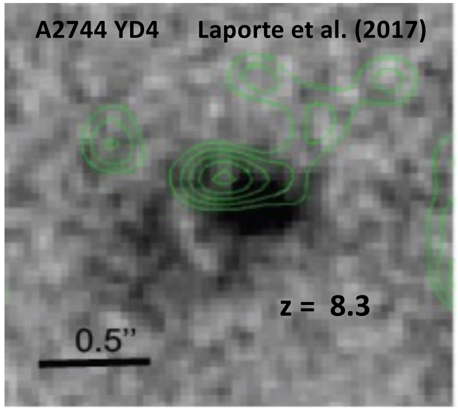

M_{star} ~ 2 10^9 M_{sun} SFR ~ 20 M_{sun}/yr
M_{dust} ~ 6 10^6 M_{sun}

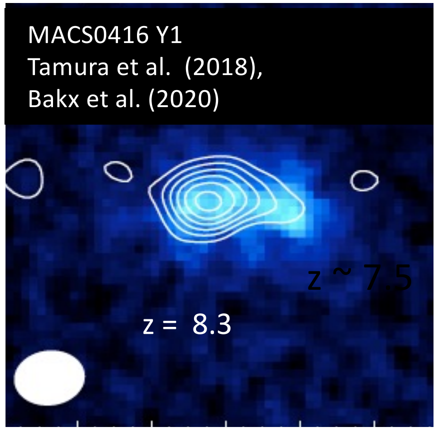

M_{star} ~ (0.3 – 1) 10^{10} M_{sun}
SFR ~ 60 M_{sun}/yr
M_{dust} ~ (7.7 10^6 – 6 10^4) M_{sun}

A1689-zD1   Knudsen et al. (2017)

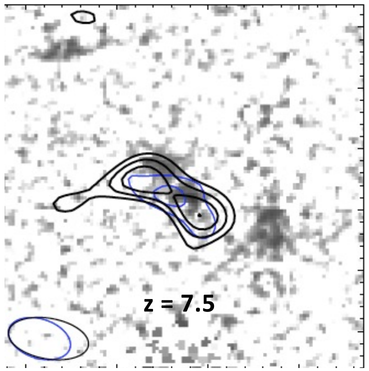

B14-65666   Hashimoto et al. 2018

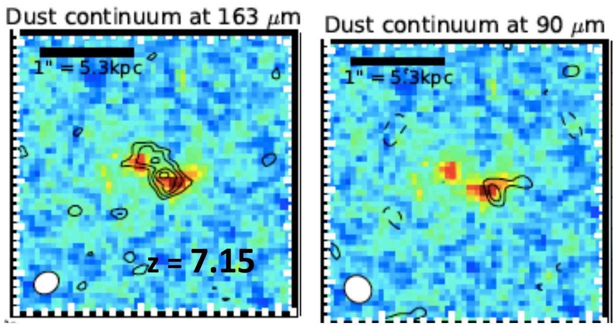

M_{star} ~ 2.1 10^9 M_{sun} SFR ~ 143 M_{sun}/yr
M_{dust} ~ (1 – 6) 10^7 M_{sun}

Bowler et al. 2018

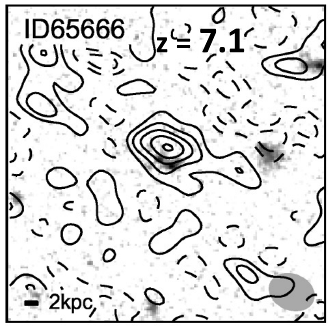

M_{star} ~ 10^9 M_{sun} SFR ~ 50 M_{sun}/yr
M_{dust} ~ 2 10^7 M_{sun}

the dust mass in “normal” SF galaxies at z ≈ 6

Shimizu+14; Mancini, RS+2015, 2016; Khakaleva-Li & Gnedin 2016; Zhukowska+ 2016; Grassi+ 2016; McKinnon+ 2016
Aoyama+2016; Graziani+ 2020

the dust mass in some “normal” galaxies at 5 < z < 8.4 compared to local galaxies

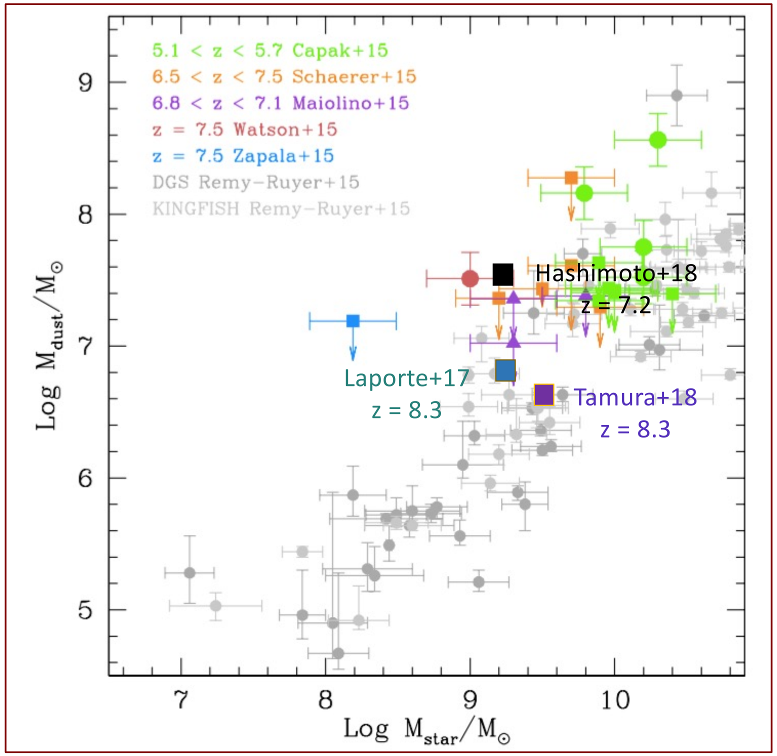

“normal” star forming galaxies at z > 6 have a dust-to-stellar mass relation consistent with local galaxies

REBELS
Reionization Era Bright Emission Line Search

ALMA REBELS Survey

ALMA Large Program targeting 40 UV bright star forming galaxies at z > 6.5 performing spectral scans of the CII and OIII emission lines

redshift distribution

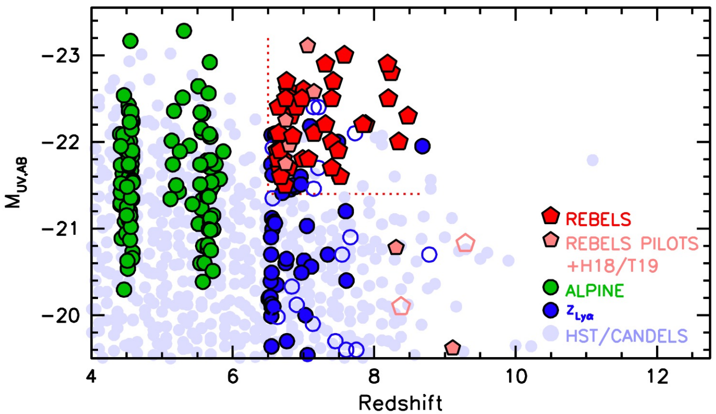

Bouwens+2022

dust continuum detected sources

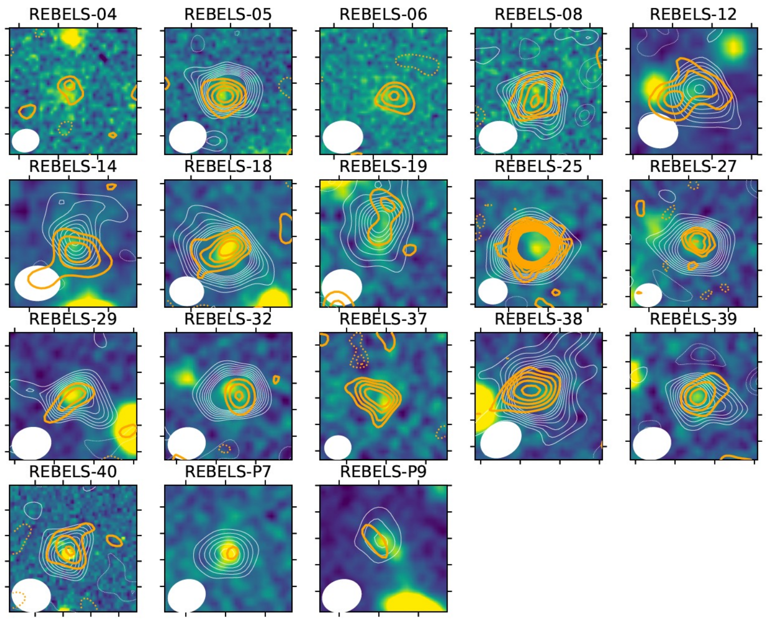

Inami et al. (2022)

dust obscured serendipitous sources

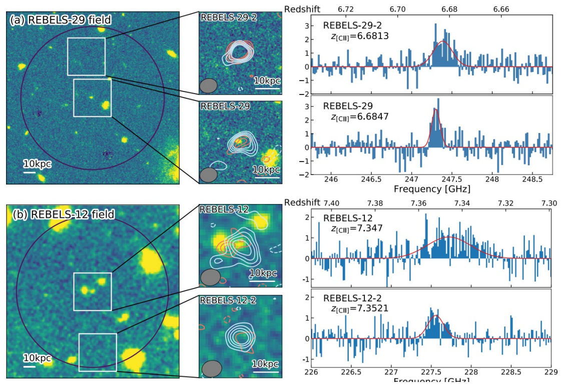

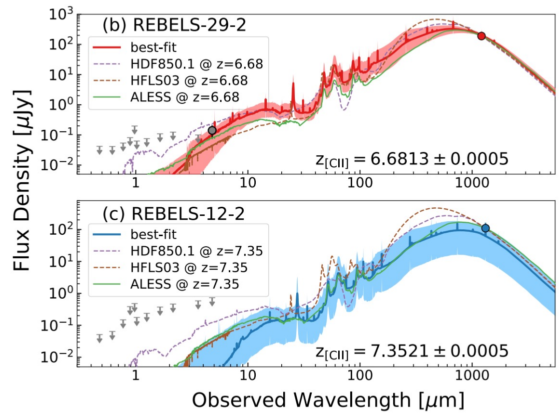

Fudamoto et al. (2021)

dust mass budget

dust yield per SN and AGB stars required to explain the observed dust masses

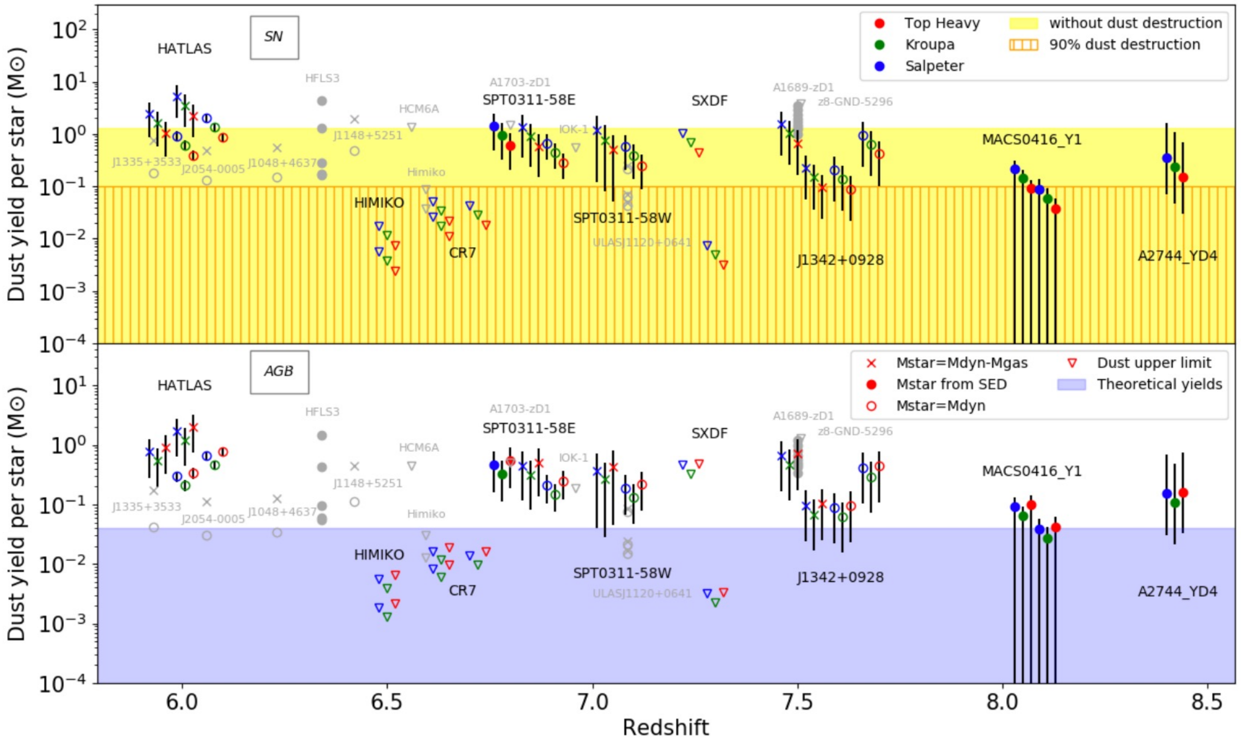

Michałowski et al. 2010; Michałowski 2015; Lesniewska & Michałowski (2019)

“the observed amounts of dust in the galaxies in the early universe were formed either by efficient supernovae or by a non-stellar mechanism, for instance the grain growth in the interstellar medium”

dustyGadget: simulating dust enrichment in the EoR

Graziani, RS et al. (2020)

On the fly dust production/ISM processing:

- ❖ SN/AGB dust production $y_d(m,Z)$
- ❖ ISM grain growth $\boldsymbol{\tau}(n,T,Z)$
- ❖ destruction in SN shocks
- ❖ sublimation in the hot phase
- ❖ astration/ejection in outflows

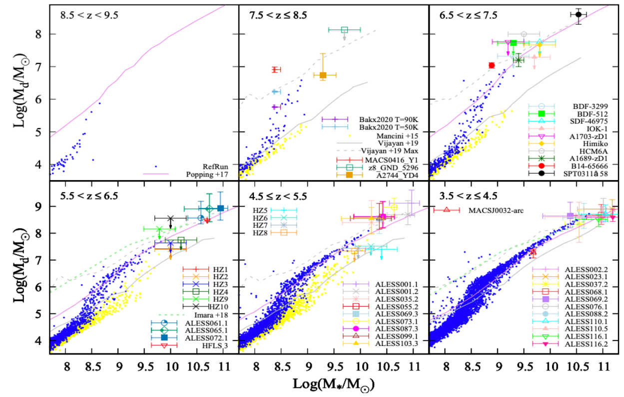

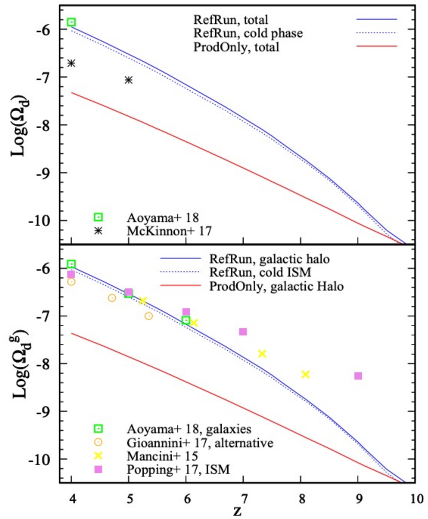

set of 8 independent cosmological simulations

L_{box} = 50 h^{-1} Mpc and $N_p = 2x533^3$

m_{dm} = 2.97 10^7 h^{-1} M_{sun}

Di Cesare, Graziani, RS et al. (2022)

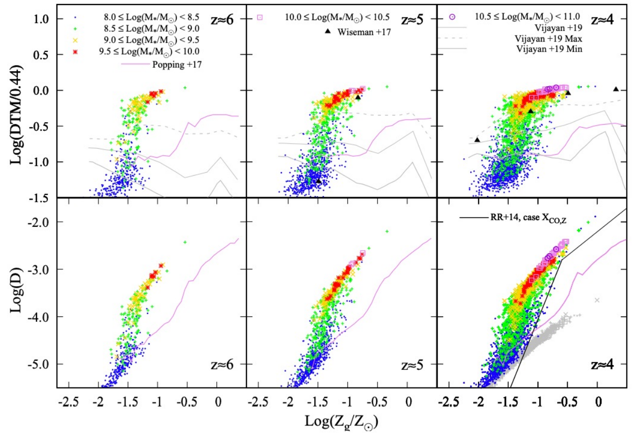

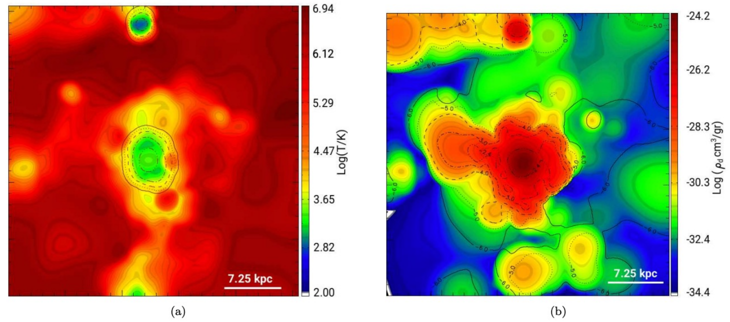

dust masses from multiband photometry

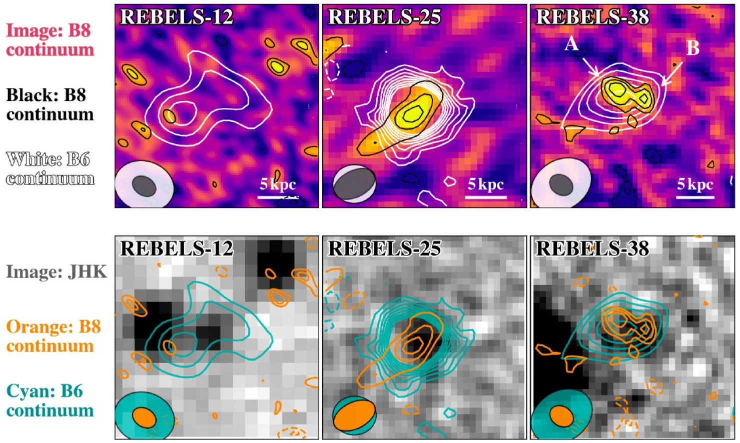

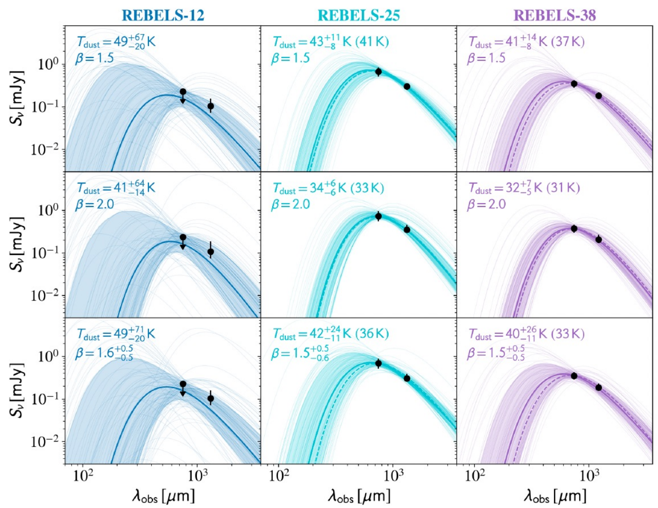

Algera and the REBELS, 2023

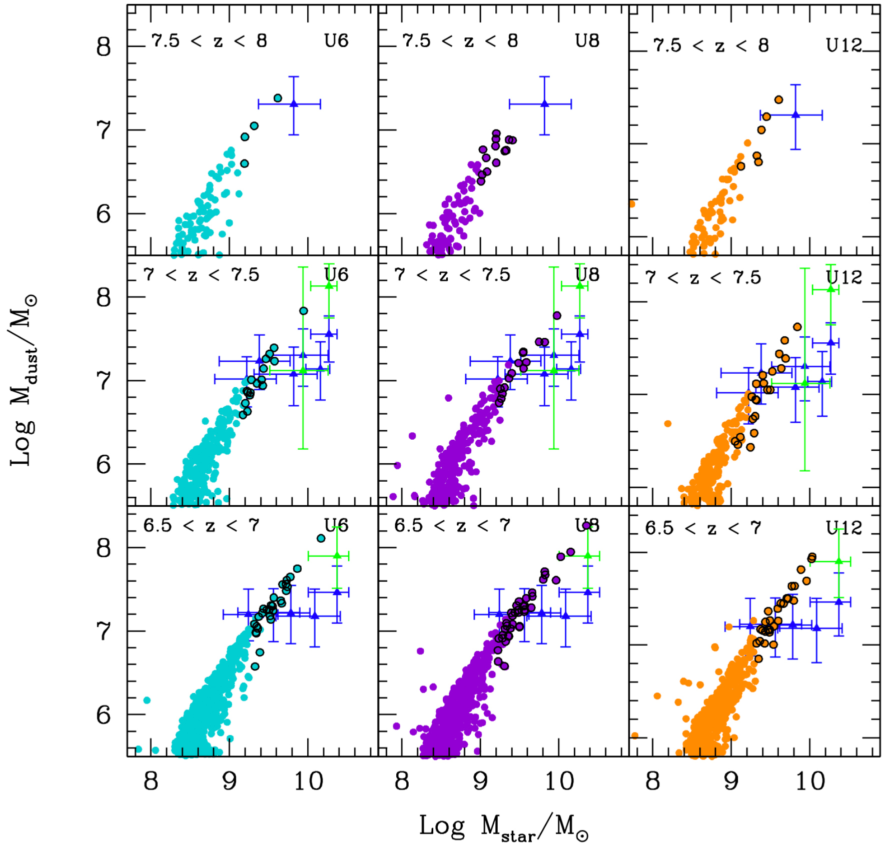

RS, Graziani and the REBELS, in prep

rapid dust enrichment in the first galaxies

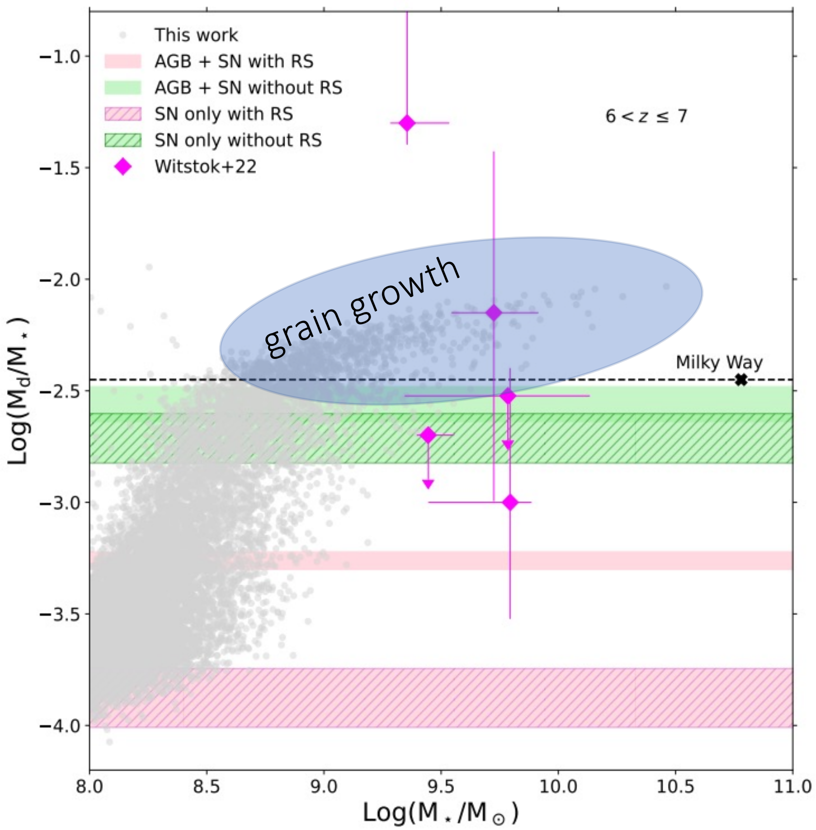

Di Cesare, Graziani, RS et al. (2022)

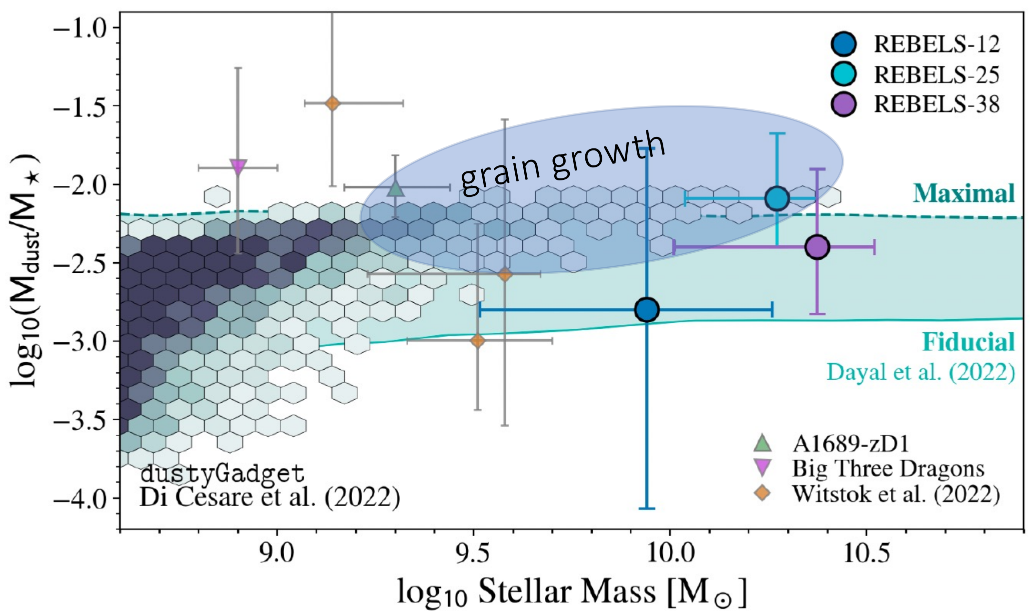

Algera and the REBELS (2023)

see also Witstok+2023

gas and dust distributions in selected systems at z ≈ 6.7

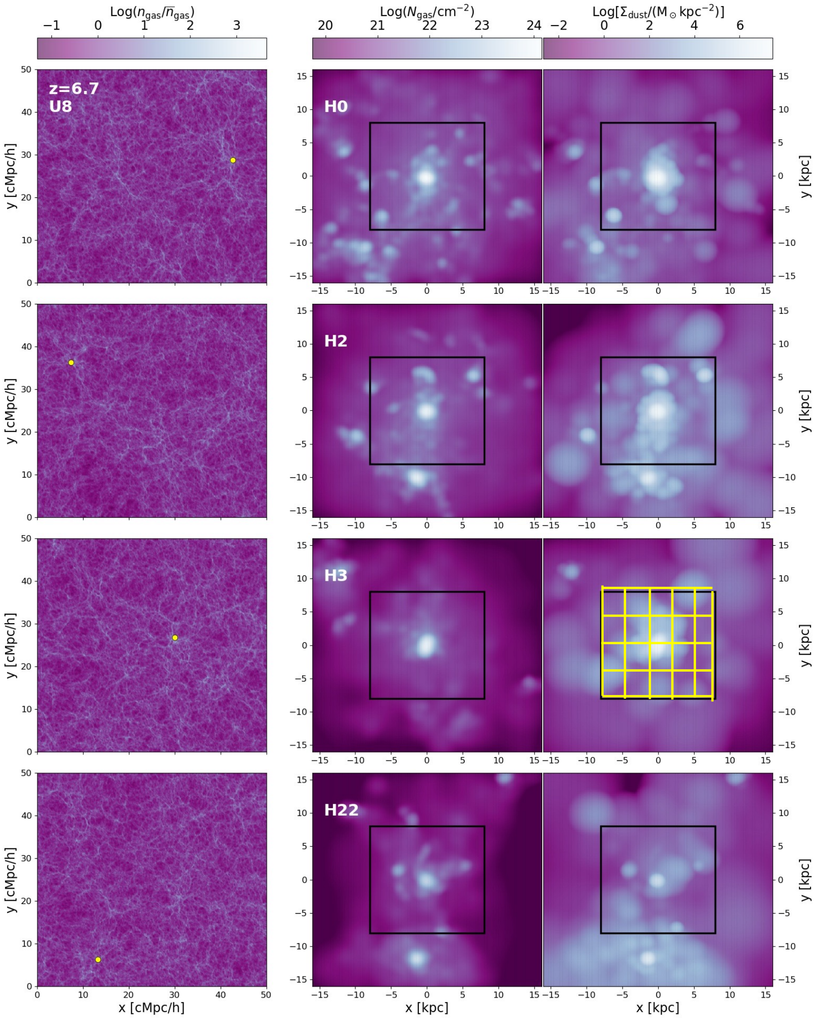

clumpy and inhomogeneous distribution that extends on kpc scales

post-process selected halos with SKIRT

N = 10^6 photon packets
256 (≈ 30 pc) cells
SMC-like dust
Starburts99 SPS (Z_{star}, t_{age})

Credits: Alessandra Venditti

dust temperature: colder than expected?

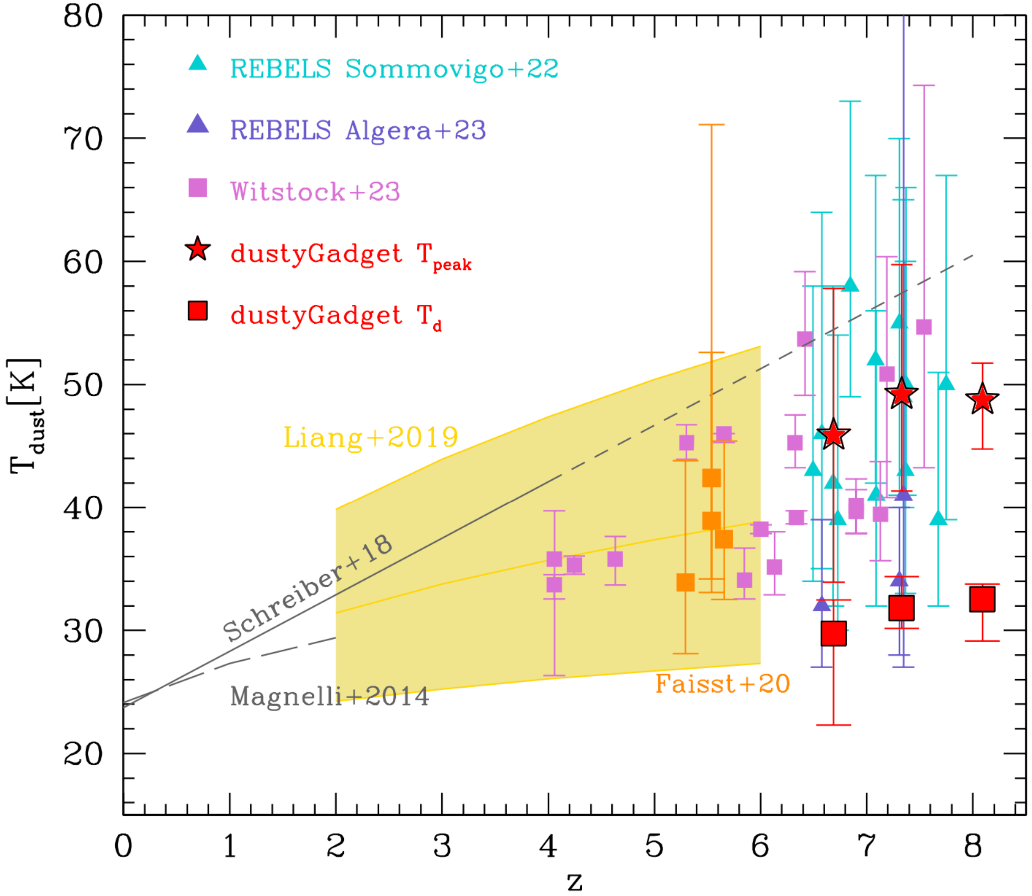

RS, Graziani and the REBELS, in prep

very mild increase in dust temperature with z at 6.5 < z < 8

mass-weighted average $T_d \approx 20$ K colder than T_{peak}

see also Sommovigo+22

empirical study of dust properties at 4 < z < 8

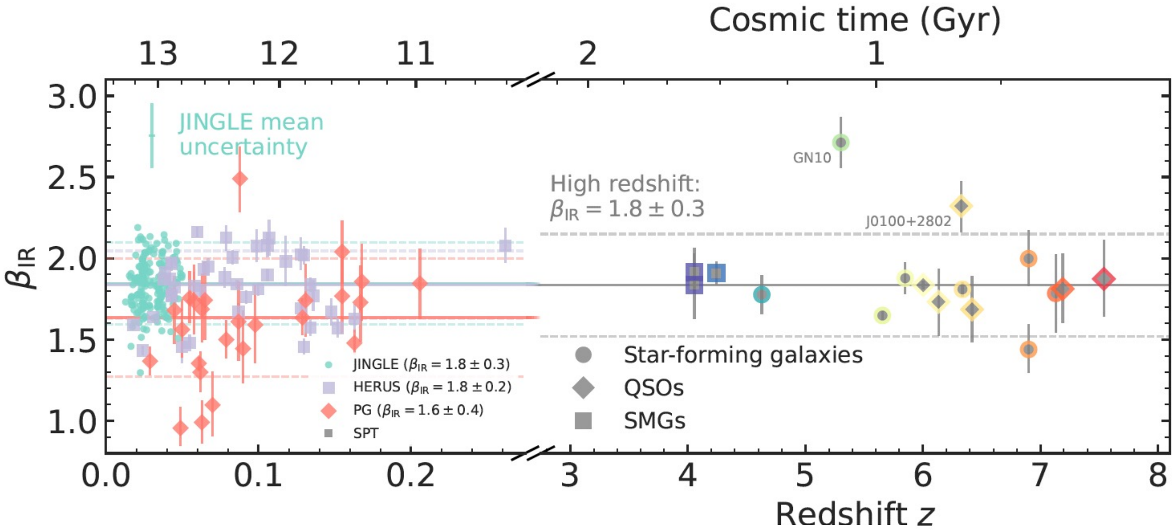

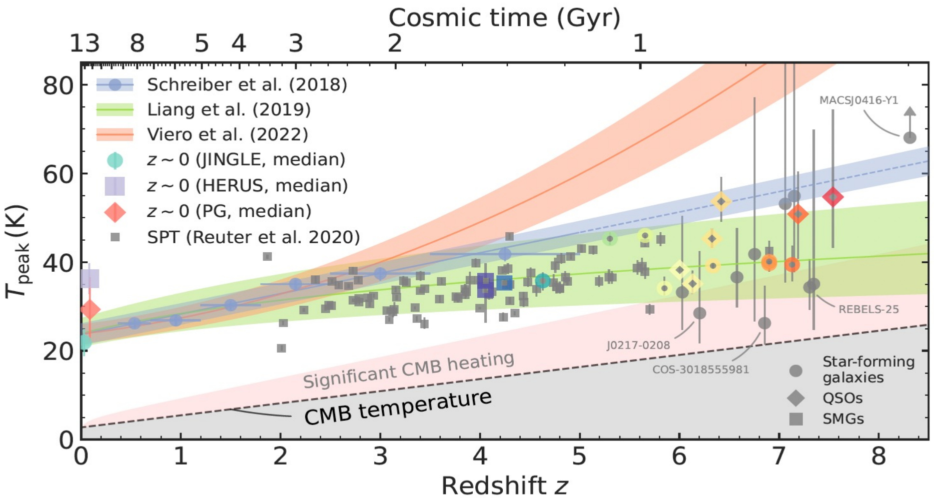

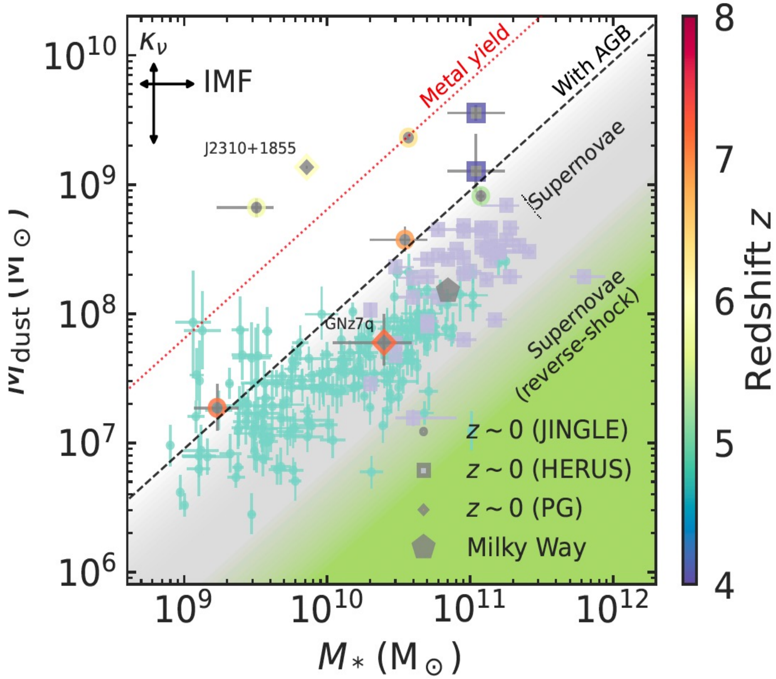

Witstok et al. (2023)

dust composition at the earliest cosmic epochs

all stars are formed in a burst

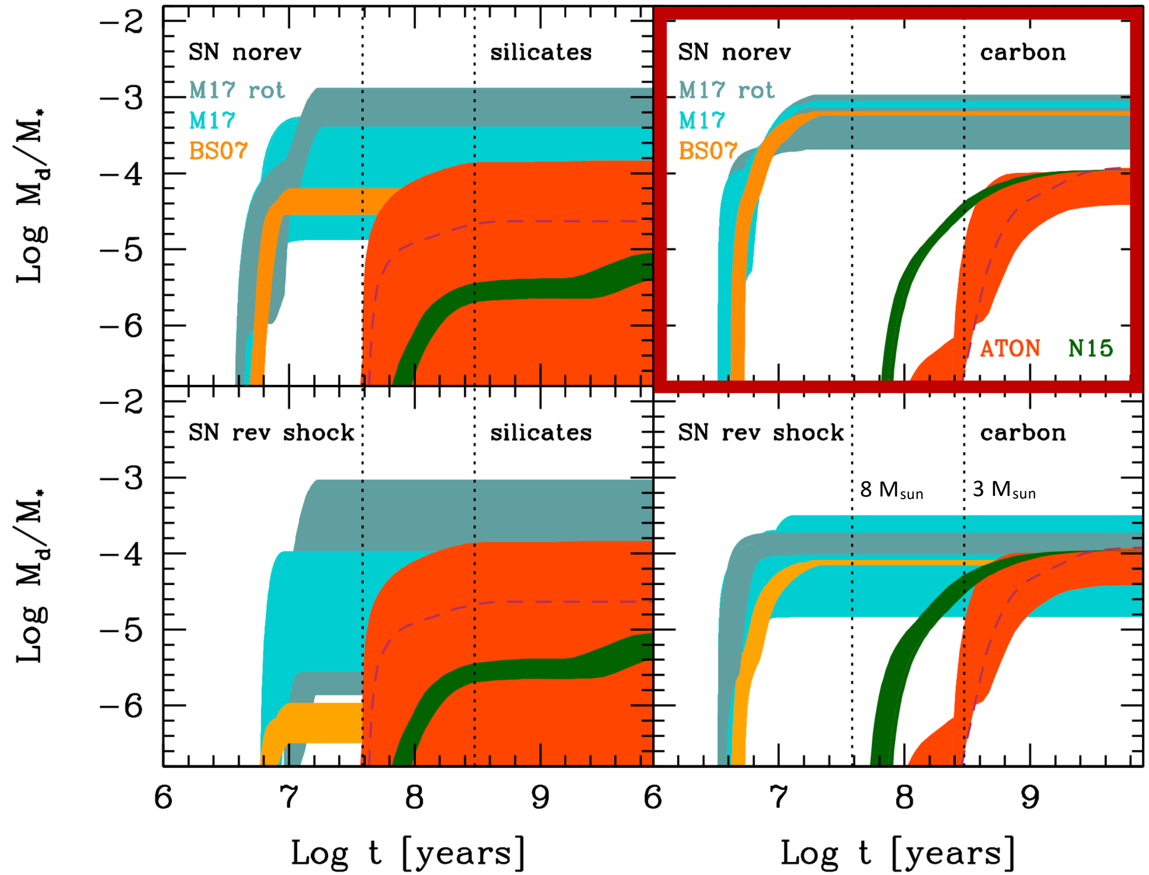

carbon dust production is dominated by supernovae if stars are younger than 300 Myr

RS & Maiolino, A&A review 2024

dust composition at the earliest cosmic epochs

2175 A carbonaceous dust absorption feature in JWST spectrum of the **z ≈ 6.71 galaxy JADES-GS-z6-0**
Log M_{star}/M_{sun} ≈ 8, SFR ≈ 2 M_{sun}/yr, Z ≈ 0.2 Z_{sun}, **t* ≈ 30 Myr**

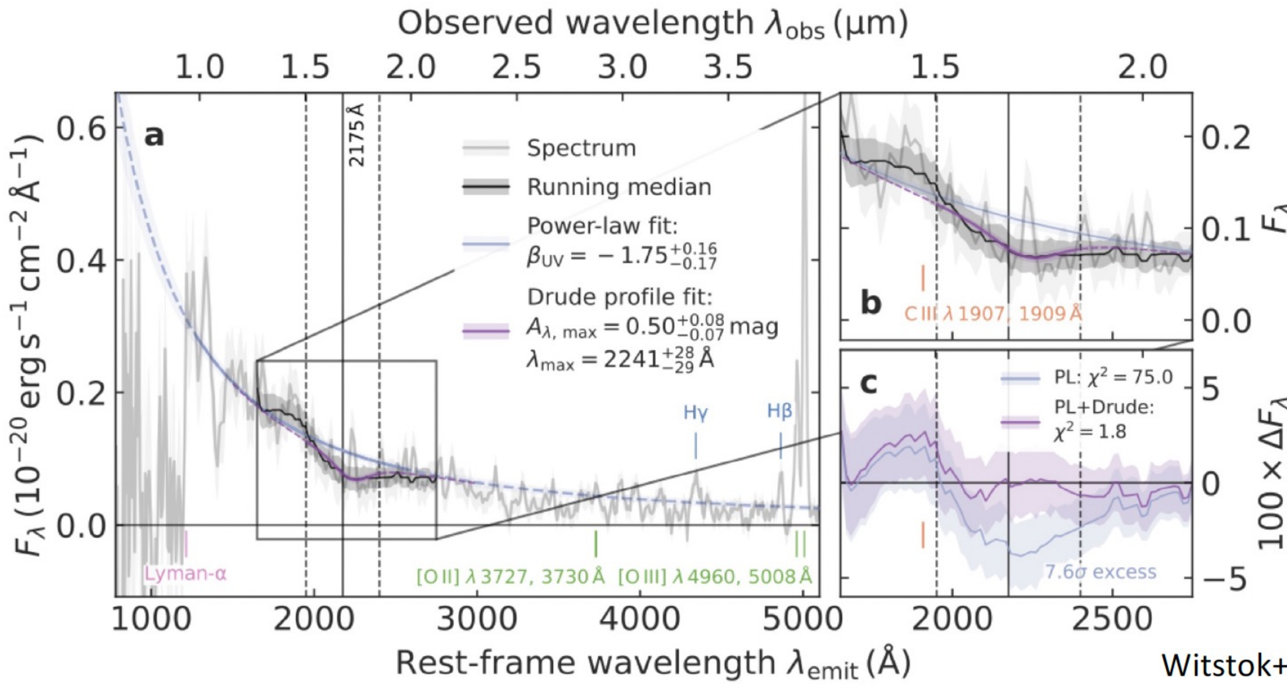

Witstok+23

direct evidence of supernova
dust production in the early Universe

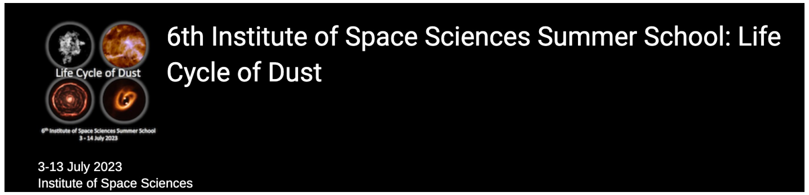

Summary and take-home messages

- dust grains form at the end of stellar evolution: AGB stars and SNe
- dust yields depend on poorly constrained parameters & importance of SN reverse shock (stellar evolution and nucleation theory)
- the relative importance of AGB stars and SNe as dust factories depends on: the stellar initial mass function, the star formation history and metallicity
- the dust content is different in different phases of the ISM as a consequence of grain processing by SN-shocked gas and grain growth in dense metal-enriched clouds
- due to the short destruction timescales, grain growth is a fundamental source of dust in the MW and it is required to reproduce observed dust-to-gas scaling relations

Summary and take-home messages

- observations at mm wavelengths show that quasar host galaxies at $z > 6$ are highly dust-enriched
- "normal" star forming galaxies at $z > 6$ have a dust-to-stellar mass relation consistent with local galaxies
- stellar dust is dominant at $M_{star} < 10^8\ M_{sun}$ and grain growth is efficient at larger masses
- vastly different dust content of local metal-poor dwarfs at comparable Z suggests that density plays an important role in the grain growth timescale
- the chemical maturity of $z > 6$ galaxies suggests that early metal and dust enrichment may have been more efficient than previously thought, possibly requiring favorable ISM conditions for SN productions and grain growth

Bibliography

Introduction to astrophysical dust:

Draine 2003, ARAA, 41, 241

http://adsabs.harvard.edu/abs/2003ARA%26A..41..241D

AGB dust production:

Schneider* et al. 2015, ASPC, 497, 369 and references therein

http://adsabs.harvard.edu/abs/2015ASPC..497..369S

*this is a proceeding where we collect the results published in a series of papers

SN dust production:

Bianchi & Schneider 2007, MNRAS, 378, 973

http://adsabs.harvard.edu/abs/2007MNRAS.378..973B

Marassi, S. 2015, MNRAS, 454, 4250

http://adsabs.harvard.edu/abs/2015MNRAS.454.4250M

Bocchio M. 2016, A&A, 587, A157

https://ui.adsabs.harvard.edu/abs/2016A%26A...587A.157B/abstract

Cosmic dust yield:

Valiante R. et al. 2009, MNRAS, 397, 1661 (first part)

http://adsabs.harvard.edu/abs/2009MNRAS.397.1661V

Lifecycle of dust in the interstellar medium of the MW:

de Bennassuti M. et al. 2014, MNRAS, 445, 3039

http://adsabs.harvard.edu/abs/2014MNRAS.445.3039D

Ginolfi, M. et al. 2018 MNRAS, 473, 4538

https://ui.adsabs.harvard.edu/abs/2018MNRAS.473.4538G/abstract

Dust in the most metal-poor local dwarfs: metallicity is not the only player

Schneider, Hunt, Valiante 2016, MNRAS, 457, 1842

http://adsabs.harvard.edu/abs/2016MNRAS.457.1842S

Bibliography

High-z observations at mm wavelengths:

Casey, Narayanan, Cooray 2014 Physical Reports, 541, 45

http://adsabs.harvard.edu/abs/2014PhR...541...45C

Carilli & Walter 2013, ARAA, 51, 105

http://adsabs.harvard.edu/abs/2013ARA%26A..51..105C

Inami et al. 2022, MNRAS, 515, 3126

https://ui.adsabs.harvard.edu/abs/2022MNRAS.515.3126I/abstract

Fudamoto et al. 2021, Nature, 597, 489

https://ui.adsabs.harvard.edu/abs/2021Natur.597..489F/abstract

Witstok et al. 2023, MNRAS, 523, 3119

https://ui.adsabs.harvard.edu/abs/2023MNRAS.523.3119W/abstract

The origin of dust in high-z quasar hosts:

Valiante et al. 2014, MNRAS, 444, 2442

http://adsabs.harvard.edu/abs/2014MNRAS.444.2442V

The origin of dust in high-z “normal” star forming galaxies

Mancini, M. 2015, MNRAS, 451, L70

http://adsabs.harvard.edu/abs/2015MNRAS.451L..70M

Graziani, L. et al. 2020, MNRAS, 494, 1071

https://ui.adsabs.harvard.edu/abs/2020MNRAS.494.1071G/abstract

Di Cesare et al. 2023, MNRAS, 519, 4632

https://ui.adsabs.harvard.edu/abs/2023MNRAS.519.4632D/abstract

The formation and cosmic evolution of dust - I: dust sources

Raffaella Schneider · Roberto Maiolino

The formation and cosmic evolution of dust - II: cosmic dust at $z > 4$

Roberto Maiolino · Raffaella Schneider